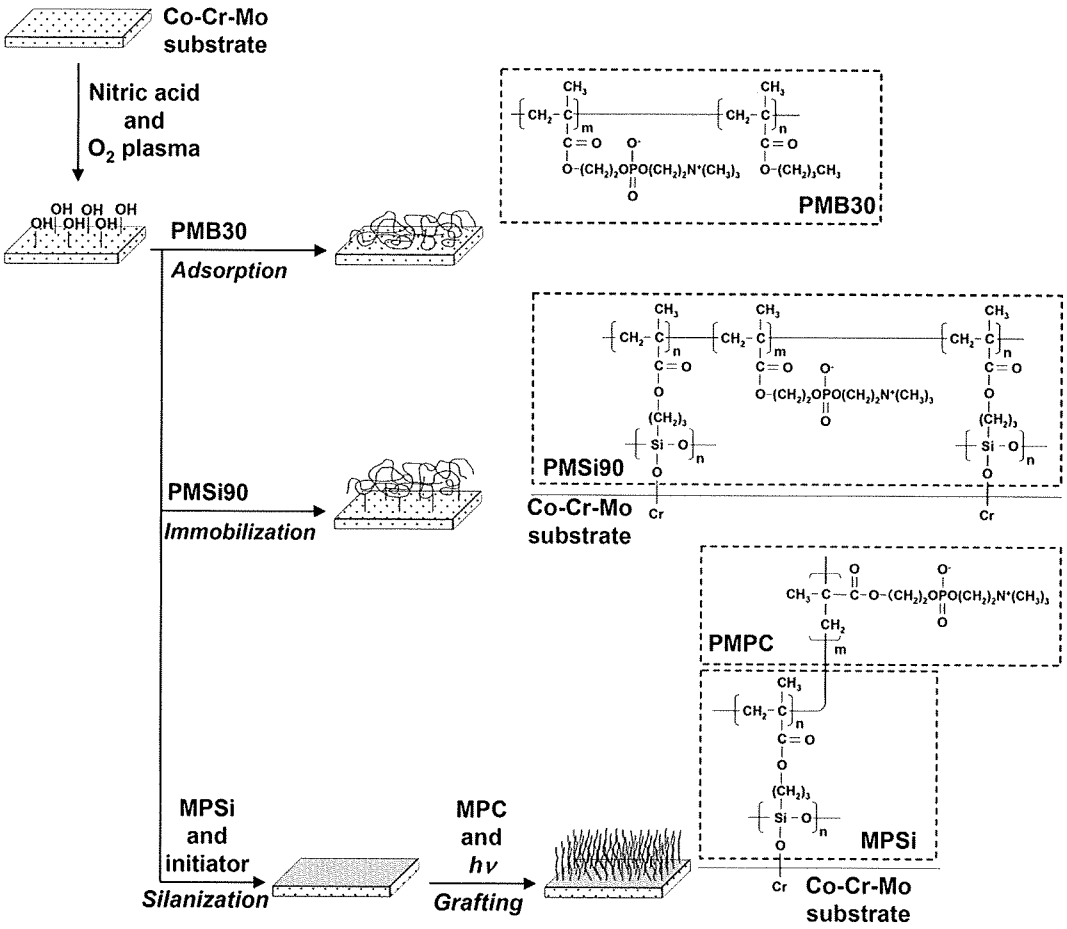

Fig. 1. Schematic illustration for the preparation of MPC polymer-coated and PMPC-grafted Co–Cr–Mo.

2.7. Cross-sectional observation by transmission electron microscopy

A cross-section of the surface-modified Co–Cr–Mo samples was observed using a transmission electron microscope (TEM) and by energy dispersive X-ray (EDX) spectroscopy. The specimens were precoated with an aluminum film; then, a thin film of the samples was prepared by the focused ion beam (FIB) technique using an FB-2000A (Hitachi High-Technologies Co., Tokyo, Japan) FIB system. The samples were thinned to electron transparency by a low gallium ion beam current. The thin film thus prepared was positioned onto a copper TEM mesh grid. TEM observations were then recorded using an HF-2000 electron microscope (Hitachi High-Technologies Co.) at an acceleration voltage of 200 kV. EDX spectra were analyzed on a cross-section of the samples using a Sigma EDX attachment (Kevex Instruments, Inc., Valencia, CA, USA) at an acceleration voltage of 200 kV.

2.8. Characterization of protein adsorption by micro bicinchoninic acid method

The amounts of protein adsorbed on the surface-modified Co–Cr–Mo samples were determined by the micro bicinchoninic acid (BCA) method. Each specimen was immersed in PBS for 1 h to equilibrate the surface modified by the MPC polymer. The specimens were immersed in bovine serum albumin (BSA, Mw = 6.7×10^4; Sigma–Aldrich Corp., MO, USA), bovine blood γ-globulins (Mw = 1.5×10^5; Sigma–Aldrich Co.), and bovine plasma fibrinogen (Mw = 3.4×10^5; Sigma–Aldrich Co.) solutions at 37 °C for 1 h. The protein solutions were prepared in BSA, γ-globulins, and fibrinogen concentrations of 4.5, 1.6, and 0.3 g/L, respectively, i.e., 10% of the concentration of human plasma levels. Then, the specimens were rinsed five times with fresh PBS and immersed in 1 mass% sodium dodecyl sulfate (SDS) aqueous solution and shaken at room temperature for 1 h to completely detach the adsorbed BSA, γ-globulins, and fibrinogen on the surface modified by the MPC polymer. A protein analysis kit (micro BCA protein assay kit, #23235; Thermo Fisher Scientific Inc., IL, USA) based on the BCA method was used to determine the BSA concentration in the SDS solution, and the amount of BSA, γ-globulins, and fibrinogen adsorbed on the surface modified by the MPC polymer was calculated.

2.9. Friction test and histological observation of articular cartilage

The coefficients of dynamic friction between the pins fabricated from articular cartilage and the surface-modified Co–Cr–Mo plates were measured by using a pin-on-plate machine (Tribostation 32; Shinto Scientific Co., Ltd., Tokyo, Japan). The friction tests were performed at room temperature and 37 °C with various loads in the range from 0.49 to 9.80 N, sliding distance of 25 mm, and frequency of 1 Hz for a maximum of 5×10^3 cycles [21]. Pure water, mixture of 25 vol% bovine serum (BS), 20 mM/L of ethylene diamine tetraacetic acid (EDTA), 0.1 mass% sodium azide, and the BS mixture containing 0.02 mass% MPC polymer (PMB30 (Mw = 5.0×10^4), PMSi90 (Mw = 9.8×10^4), and PMPC (Mw = 1.0×10^5)) were used as a lubricant each. Subsequently, five replicate measurements were performed for each sample, and the average values were regarded as the coefficients of dynamic friction. After 100 cycles of friction tests, the plate samples were FM-observed. Then, after 5×10^3 cycles friction test, articular cartilage pins against the untreated Co–Cr–Mo and PMPC-grafted Co–Cr–Mo were fixed with 10% neutral buffered formalin for 3 d, then decalcified in KC-X solution (Falma Co., Tokyo, Japan) for 8 d, and then dehydrated in graded ethanol for histological observation. The decalcified cartilage specimens were embedded in paraffin (Tissue-prep; Fisher Scientific Corp., Fair Lawn, NJ, USA), and microsections were prepared and stained with hematoxylin (Real hematoxylin; Dako Co., Carpinteria, CA, USA) and eosin (Eosin yellowish; Kanto Chemical Co., Inc.) (H&E) as well as with Safranin O (Nacalai Tesque, Inc., Kyoto, Japan) and observed with a microscope (Eclipse E600; Nikon Corp., Tokyo, Japan) equipped with a CCD camera (DP72; Olympus Co., Tokyo, Japan).

2.10. PBS soaking test

The surface-modified Co–Cr–Mo samples (10 × 10 × 1 mm^3 in size) were soaked in 50 mL of PBS. After soaking with 120 rpm shaking at 37 °C for 1, 4, 8, and 12 weeks, the samples removed from the PBS and were characterized by XPS analysis, water-contact angle measurement, and FM observation.

Table 1
Surface elemental composition ($n = 5$) and static-water contact angle ($n = 15$) of untreated, MPC polymer-coated and PMPC-grafted Co–Cr–Mo alloy.

Sample	Surface elemental composition (atom%)								Contact angle (deg)
	C_{1s}	O_{1s}	N_{1s}	P_{2p}	Si_{2p}	Co_{2p}	Cr_{2p}	Mo_{3d}	
Co–Cr–Mo (untreated)	14.6	52.9	0.0	0.0	0.0	26.7	5.4	0.4	81.6
	(1.3)[a]	(2.7)	(0.0)	(0.0)	(0.0)	(1.5)	(0.4)	(0.0)	(4.8)
PMB30-adsorbed Co–Cr–Mo	70.6	24.1	2.3	3.0	0.0	0.0	0.0	0.0	95.8[b]
	(1.4)	(1.3)	(0.4)	(0.3)	(0.0)	(0.0)	(0.0)	(0.0)	(3.5)
PMSi90-immobilized Co–Cr–Mo	61.4	29.5	3.6	4.2	1.3	0.1	0.0	0.0	16.6[b]
	(0.9)	(0.7)	(0.4)	(0.1)	(0.4)	(0.2)	(0.0)	(0.0)	(2.4)
PMPC-grafted Co–Cr–Mo	61.7	28.0	5.0	5.3	0.1	0.0	0.0	0.0	23.5[b]
	(0.7)	(0.6)	(0.3)	(0.1)	(0.1)	(0.0)	(0.0)	(0.0)	(8.4)

[a] The standard deviations are shown in parentheses.
[b] Significant difference ($p < 0.001$) as compared to the untreated Co–Cr–Mo.

2.11. Statistical analysis

The results derived from each measurement in the water-contact angle measurement, friction test, and protein adsorption test were expressed as mean values ± standard deviation. The statistical significance ($p < 0.05$) was estimated by Student's *t*-test.

3. Results

Fig. 2 shows the FT-IR/ATR spectra of the surface-modified Co–Cr–Mo samples with various MPC polymers. Absorption peaks were newly observed for the surface-modified Co–Cr–Mo with MPC polymers. The peaks at 1720, 1550, and 1460 cm^{-1} are attributed to C = O and -CH_2- in the MPC polymer. The peaks at 1180, 1040, 700, and 630 cm^{-1} are attributed to the trimethoxysilane group in the MPSi unit [19]. The peaks at 1240, 1080, 970, and 920 cm^{-1} are attributed to the $-N^+(CH_3)_3$ and phosphate groups in the MPC unit [22]. The absorption peak intensities of the phosphate groups of the PMPC-grafted Co–Cr–Mo were the highest in the Co–Cr–Mo whose surface was modified by the MPC polymer.

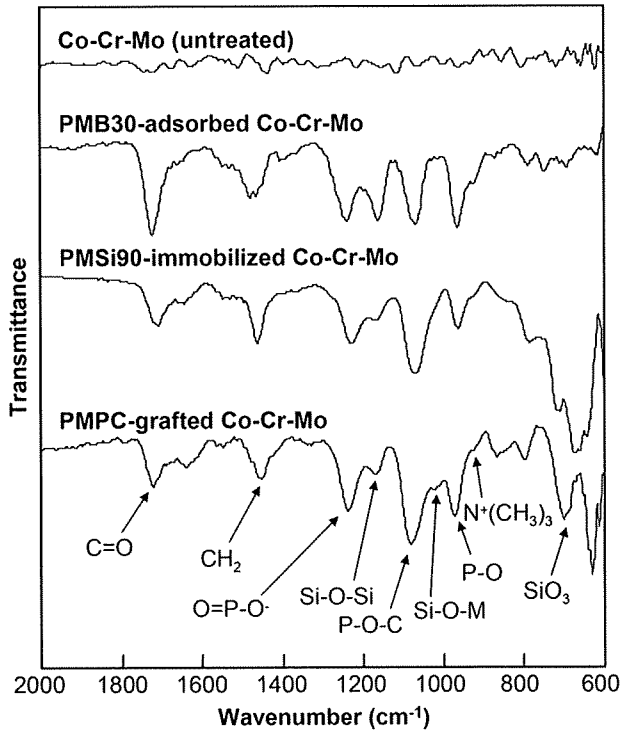

Fig. 2. FT-IR/ATR spectra of untreated Co–Cr–Mo, MPC polymer-coated Co–Cr–Mo, and PMPC grafted Co–Cr–Mo.

Table 1 summarizes the surface elemental composition and static-water contact angle of the surface-modified Co–Cr–Mo samples with various MPC polymers. The nitrogen (N) and phosphorous (P) contents in all the Co–Cr–Mo samples whose surfaces were modified by the MPC polymer were observed. The elemental compositions of both N and P in the surface-modified Co–Cr–Mo increased with an increase in the MPC composition in the polymer for surface modification. In particular, these values of N and P in the PMPC-grafted Co–Cr–Mo surface were 5.0 and 5.3 atom%, respectively, and were almost equivalent to the theoretical elemental composition (N = 5.3, P = 5.3 atom%) of PMPC. The static-water contact angle of the untreated Co–Cr–Mo was 81.6°, and this decreased markedly to approximately 20° (i.e., 16.6°–23.5°, $p < 0.001$) by the modifications with PMSi90 and PMPC.

Fig. 3 shows the cross-sectional TEM images of the surface-modified Co–Cr–Mo samples with various MPC polymers. For PMB30-adsorption, PMSi90-immobilization, and PMPC-grafting, a thickness of 50, 130, and 200 nm, respectively, of the MPC polymer layers was clearly observed on the surface of the Co–Cr–Mo substrate. No cracks due to poor adhesion and/or delamination were observed at the interface between the MPC polymer layer and Co–Cr–Mo substrate. These results indicate that each surface modification layer on the Co–Cr–Mo substrate is uniform and adheres closely, regardless of the binding conditions; the surface modification layers by PMB30-adsorption, PMSi90-immobilization, and PMPC-grafting combine with the substrate by physical adsorption and covalent bonds of Si–O–metal (M), respectively. However, in the PMB30-adsorbed Co–Cr–Mo, a bilayer structure for poor adhesion attributed to dipping twice was clearly observed on the surface modification layer. Further, in the PMB30-adsorbed and PMSi90-immobilized Co–Cr–Mo samples, a porous structure was clearly observed on the surface modification layer. This porous structure was also observed on the surface modification layer prepared by the slow-rate solvent evaporation method (approximately for 1 month at 4 °C, data not shown).

Fig. 4 shows the EDX spectra of the surface-modified Co–Cr–Mo samples with various MPC polymers. In spectra (b_{1-3}), (c_{1-3}), and (d_{1-3}) of the MPC polymer layers, a significant peak attributed to the P atom was observed at 2.0 keV. This peak is mainly attributed to the MPC units. Interestingly, this peak was clearly observed in spectra (b_2) and (c_2) of the porous part of the MPC polymer layer. In spectra (c_1) and (d_1) of the interface of the PMSi90-immobilization layer and the intermediate layer of the PMPC-grafted Co–Cr–Mo, peaks were observed at 0.5 and 1.7 keV. These peaks are attributed to the O and Si atoms in the interface/intermediate layer between the silane of the MPSi and the metal oxide of the Co–Cr–Mo.

Fig. 5 shows the amounts of BSA, γ-globulins, and fibrinogen adsorbed on the surface-modified Co–Cr–Mo samples with various

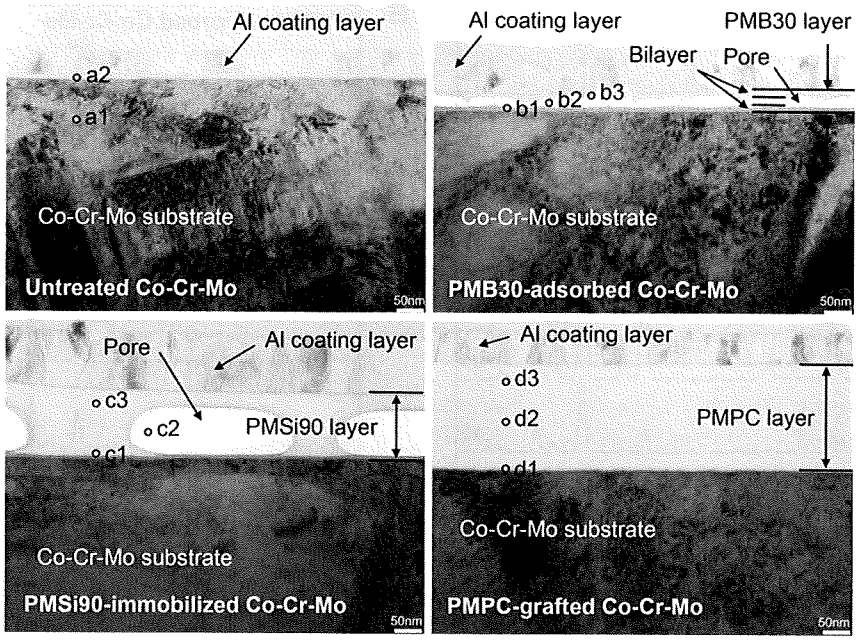

Fig. 3. Cross-sectional TEM images of the surface-modified Co–Cr–Mo with various MPC polymers. Aluminum coating layers (approximately 70–100 nm) for the preparation of TEM observation specimen are shown above the MPC polymer layer of the Co–Cr–Mo surface. Small open circles indicate EDX analysis points. Bar: 50 nm.

MPC polymers. The amount of each protein adsorbed on the Co–Cr–Mo surface modified by the MPC polymer was considerably lower ($p < 0.001$) than that on the untreated Co–Cr–Mo. These results imply that the surface modification by the MPC polymer results in good biocompatibility.

Fig. 6 shows the coefficients of dynamic friction of the sliding couples and articular cartilage pins sliding against the surface-modified Co–Cr–Mo plates with various MPC polymers. The PMB30-adsorbed and PMSi90-immobilized Co–Cr–Mo samples showed a slightly higher friction coefficient than the untreated Co–Cr–Mo sample in water at room temperature (not significantly different); in contrast, the MPC polymer-coated Co–Cr–Mo showed a lower friction coefficient than the untreated Co–Cr–Mo in BS mixture at 37 °C ($p < 0.05$). Further, the friction coefficient of the PMPC-grafted Co–Cr–Mo decreased drastically compared with untreated Co–Cr–Mo ($p < 0.001$) and reached approximately <0.010 in both lubricant conditions, i.e., water at room temperature and the BS mixture at 37 °C; moreover, it remained almost steady. The friction coefficients of all MPC polymer-containing BS mixtures were drastically lower as compared with that of non-additive BS mixture (Fig. 6).

Fig. 7 shows the coefficients of dynamic friction of the untreated Co–Cr–Mo and PMPC-grafted Co–Cr–Mo samples as a function of the loads. At both 10 and 100 cycles, the PMPC-grafted Co–Cr–Mo sample showed a remarkably low friction coefficient of approximately 0.019 at a load of 0.49 N; this value decreased gradually and reached approximately <0.010 at a load of 9.80 N. Similarly, the friction coefficients of the untreated Co–Cr–Mo sample in the initial 10 cycles decreased gradually from 0.188 to 0.045. However, this value of the untreated Co–Cr–Mo at 100 cycles decreased to 0.082 up to loads of 1.96 N; it then gradually increased with an increase in the loads. Fig. 7B shows the friction coefficients of the untreated Co–Cr–Mo and PMPC-grafted Co–Cr–Mo samples as a function of the test durations. It was observed that the friction coefficient was significantly lower in the PMPC-grafted Co–Cr–Mo sample than in the untreated Co–Cr–Mo one. This value was almost constant throughout the 5×10^3 cycles of the friction test.

Fig. 8 shows the histological findings of the articular cartilage pins after 5×10^3 cycles of friction tests. In the cartilage against the untreated Co–Cr–Mo, the cartilage layer of the worn surface became thicker as compared with the surrounding articular cartilage of the unworn surface. In contrast, in the cartilage against the PMPC-grafted Co–Cr–Mo, the layer of the worn surface did not differ considerably from that of the unworn surface.

Fig. 9 shows the time course of the surface modification layer of the untreated, MPC polymer-coated, and PMPC-grafted Co–Cr–Mo samples during PBS soaking. The elemental compositions of both N and P in the untreated, PMB30-adsorbed, and PMPC-grafted Co–Cr–Mo samples were almost constant throughout the 12 weeks of PBS soaking. In contrast, in the PMSi90-immobilized Co–Cr–Mo sample, these values decreased gradually with the PBS-soaking duration. Similarly, the static-water contact angle of untreated, PMB30-adsorbed, and PMPC-grafted Co–Cr–Mo samples were almost constant throughout PBS soaking, whereas the values in PMSi90-immobilized Co–Cr–Mo increased gradually.

Fig. 10 shows FM images of the surface-modified Co–Cr–Mo samples with various MPC polymers before and after friction tests/PBS-soaking tests. After 100 cycles of friction tests, the MPC polymer layer was removed from the PMB30-adsorbed and PMSi90-immobilized Co–Cr–Mo sliding surfaces; in contrast, most of the PMPC-grafted Co–Cr–Mo sliding surface was covered by the PMPC layer. After 12 weeks of PBS-soaking tests, most of the MPSi90 layer was removed from the Co–Cr–Mo surface, while most of the PMB30-adsorbed and PMPC-grafted Co–Cr–Mo surface was covered stably by the MPC polymer layer.

4. Discussion

In the hemi-arthroplasty, the highly lubricious surface by a "mild treatment" with soft materials was requested with aim of preserving the degradation of the articular cartilage. In this study, we have prepared various surface modification layers formed on the Co–Cr–Mo surface by MPC polymer coating or photoinduced radical polymerization of MPC to form PMPC graft chains for

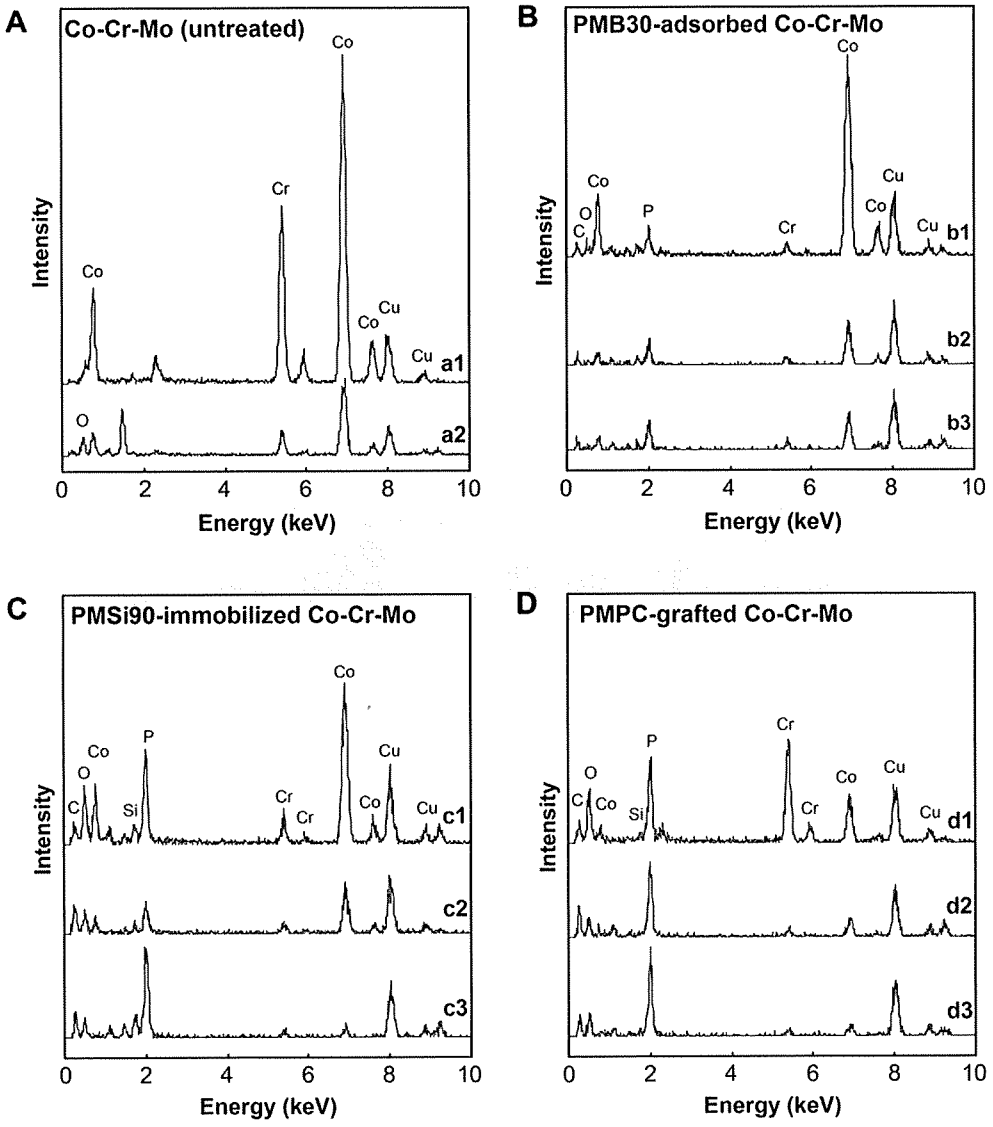

Fig. 4. EDX spectra of the untreated Co–Cr–Mo, MPC polymer-coated Co–Cr–Mo, and PMPC-grafted Co–Cr–Mo. The spectra were analyzed on the cross-section (small open circles in Fig. 3) of the untreated Co–Cr–Mo, MPC polymer-coated Co–Cr–Mo, and PMPC-grafted Co–Cr–Mo.

improving lubrication and preventing the degradation of acetabular cartilage. Here, we discuss the structures and stabilities of the surface modification layers of the MPC polymer and the effects of these characteristics on the retention of articular cartilage in hemiarthroplasty.

To ensure the *in vivo* long-term stability of the MPC modified layer on the Co–Cr–Mo surface, it is necessary to create strong covalent bonding between the Co–Cr–Mo substrate and the MPC polymer. Organosilanes have already been known as surface coupling agents that enhance bonding between a metal or a metal oxide surface and an organic resin such as dental resin; moreover, they can strongly bind metals to resins in dental implants [23]. Organic silanes or silane coupling agents comprise at least a hydrolyzable alkoxysilyl or chlorosilyl group and an organofunctional group. The agents are effective for introducing organofunctional groups into the siloxane network polymer. The organofunctional group in the silane could be useful for improving bonding with the organic overlayer. MPSi binds to the Co–Cr–Mo substrate by a condensation reaction in two steps; in the first step, MPSi is hydrolyzed (activated) and in the second step, the hydrolyzed silane molecule binds to the surface by an Si–O–M bond, forming branched hydrophobic siloxane bonds, i.e., Si–O–Si. The hydrolyzed silane molecule has three –OH groups that can react with the –OH groups of the surface metallic oxide layer to form siloxane bonds covalently. The peaks at 1180 and 1040 cm^{-1} in the FT-IR/ATR spectrum of the PMSi90-immobilized and PMPC-grafted Co–Cr–Mo surfaces were attributed to Si–O–Si and Si–O–M, respectively (Fig. 2).

However, several previous studies have reported that a silane coating has low water resistance due to hydrolysis of the siloxane bond and desorption of the physisorbed silane [24]. In fact, the PMSi90-immobilization layer was removed from the Co–Cr–Mo surface after 12 weeks of PBS soaking (Figs. 9 and 10). Zhang, et al. and others have reported that the water stability of Si–O–M could be improved by employing the following factors: (1) an induction of bridged silane coupling agents, when hydrolyzed, contain two or more $-Si(OH)_3$, (2) the hydrophobic alkyl moieties that limit the contact with water, and (3) an increase in the thickness of the

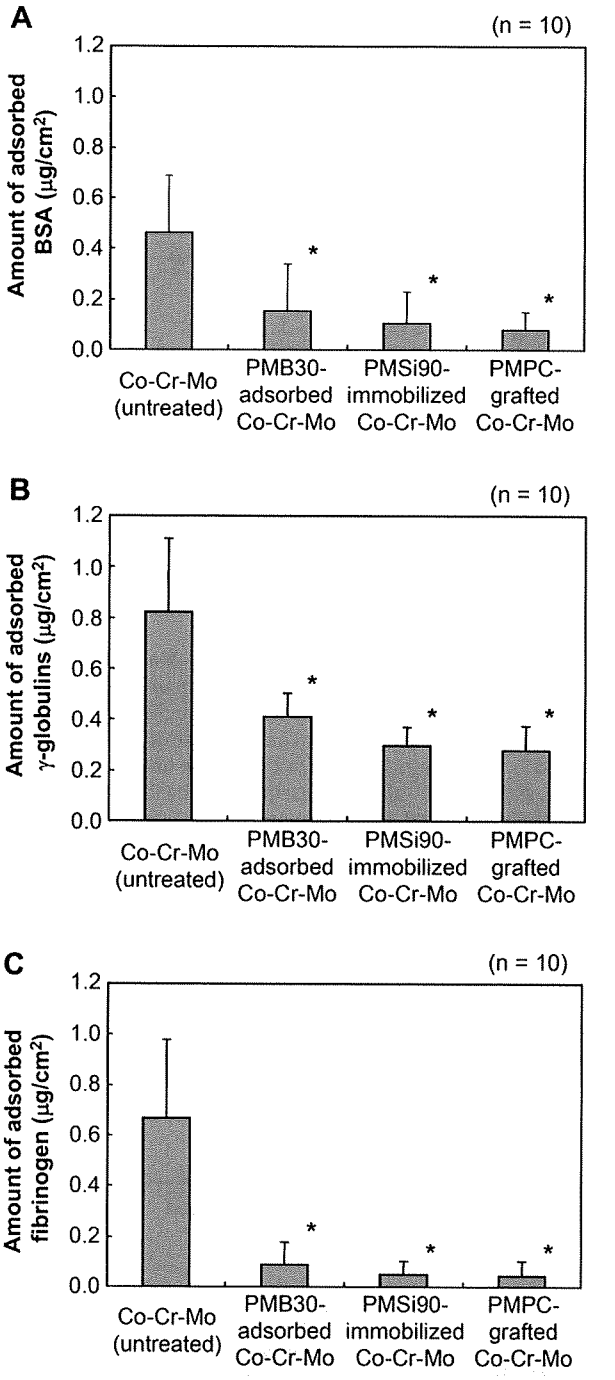

Fig. 5. Amounts of (A) BSA, (B) γ-globulins, and (C) fibrinogen adsorbed on the surfaces of the untreated Co–Cr–Mo, MPC polymer-coated Co–Cr–Mo, and PMPC-grafted Co–Cr–Mo. Bar: Standard deviations. *: Significant difference ($p < 0.001$) as compared to the untreated Co–Cr–Mo.

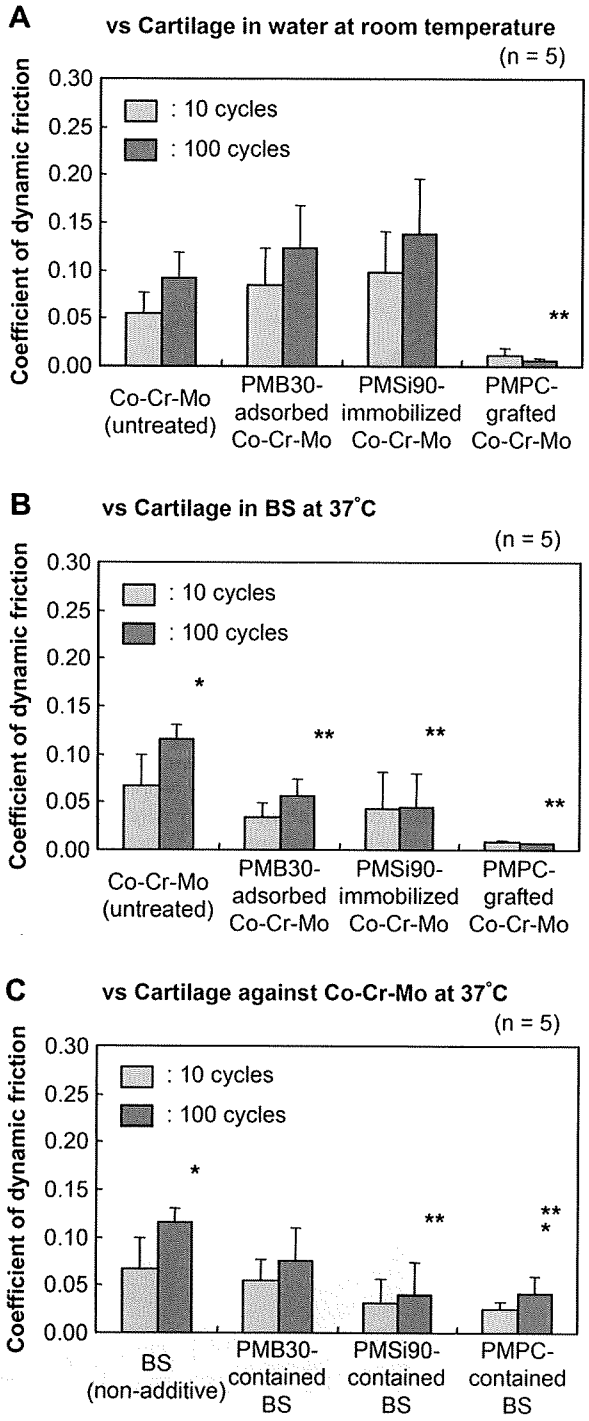

Fig. 6. Coefficients of dynamic friction of the untreated, MPC polymer-coated, and PMPC-grafted Co–Cr–Mo in the pin-on-plate friction test with various lubrication conditions. (A) Against cartilage pin with water at room temperature, (B) against cartilage pin with BS lubricant at 37 °C, (C) untreated Co–Cr–Mo plate against cartilage pin with BS lubricant with MPC polymer as additive at 37 °C. Bar: Standard deviations. *: *t*-test, significant difference ($p < 0.05$) as compared to the coefficients of dynamic friction at 10 cycles, and **: *t*-test, significant difference ($p < 0.05$) as compared to the untreated Co–Cr–Mo plate at 100 cycles.

surface oxide layer [25]. Therefore, it was considered that the MPSi intermediate layer with a bridge of three methoxysilane groups with MPSi unit composition of 100% (MPSi unit of PMSi90 composition was 10% only) was essential in PMPC-grafted Co–Cr–Mo. Additionally, a functional methacrylate and pretreatment (nitric acid treatment and O_2 plasma treatment) for the Co–Cr–Mo surface were used. As shown in Figs. 9 and 10, the high stability of

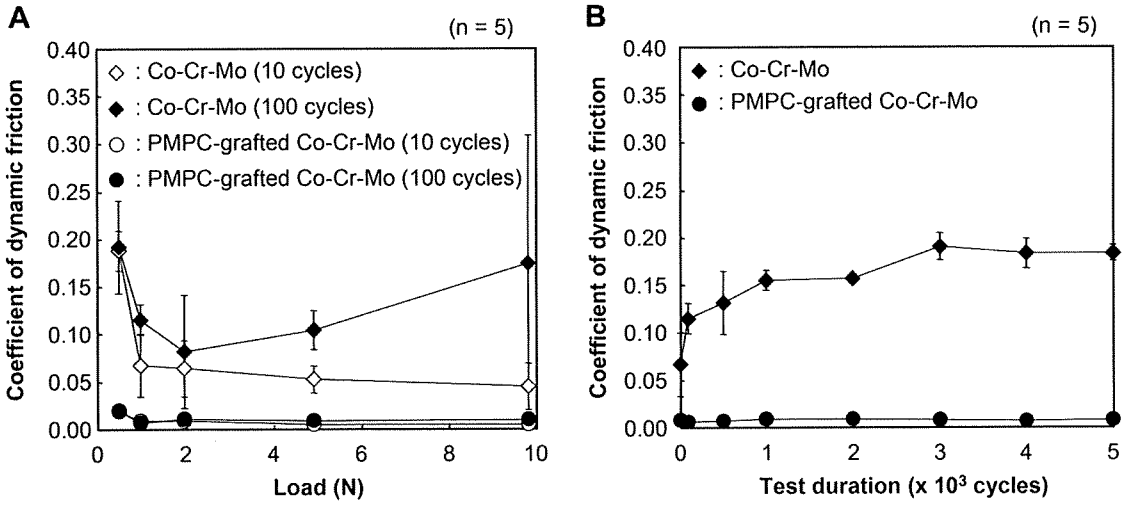

Fig. 7. Coefficients of dynamic friction of the untreated and PMPC-grafted Co–Cr–Mo in the pin-on-plate friction test. (A) Coefficients of dynamic friction of the untreated and PMPC-grafted Co–Cr–Mo against cartilage pin as a function of loads in the pin-on-plate friction test with BS lubricant at 37 °C. (B) Time course of coefficients of dynamic friction of the untreated and PMPC-grafted Co–Cr–Mo against the cartilage pin during 5×10^3 cycles of loading with 0.98 N in the pin-on-plate friction test with BS lubricant at 37 °C. Bar: Standard deviations.

the PMPC-grafted layer was confirmed throughout 12 weeks of PBS soaking.

On the other hand, the high stability of the PMB30-adsorbed layer was also confirmed throughout 12 weeks of PBS soaking. As shown in Table 1, the static-water contact angle of the PMB30-adsorbed Co–Cr–Mo was 95.8°. Sibarani et al. reported that the PMB30-adsorbed polymer surfaces showed high advancing (approximately 100°) and low receding (approximately 20°) contact angles: PMB30 cannot be hydrated easily due to the low MPC unit composition of the copolymer [10]. However, as shown in Fig. 5, the PMB30-adsorbed Co–Cr–Mo surface, which could form a phosphorylcholine-enriched surface after equilibrating for 1 h, showed excellent biocompatibility as an anti-protein adsorption surface. Hence, the PMB30-adsorbed layer has been observed to be stable (insoluble and attachable *in vivo* condition) and useful on several medical devices [14,15].

In Figs. 6 and 7, the PMPC-grafted Co–Cr–Mo surface shows an extremely low friction coefficient as compared to that of the untreated Co–Cr–Mo surface. Since MPC is highly hydrophilic and PMPC is water soluble, the water contact angle of the PMPC-grafted Co–Cr–Mo surface was lower than that of the untreated Co–Cr–Mo surface, as shown in Table 1. Consequently, the PMPC-grafted layer successfully provided high lubricity in the form of "surface gel hydration lubrication" to the Co–Cr–Mo surface (Fig. 3). A previous study has reported that the hydrogel cartilage surface is assumed to have a brush-like structure: a part of the proteoglycan brush is bonded with the collagen network on the cartilage surface [26]. The bearing surface with PMPC is assumed to have a brush-like structure similar to that of articular cartilage. Cartilage/PMPC-grafted Co–Cr–Mo bearing couples can therefore be regarded to be mimicking natural joint cartilage *in vivo*. The friction coefficient of cartilage/cartilage was reported to be approximately 0.01–0.02

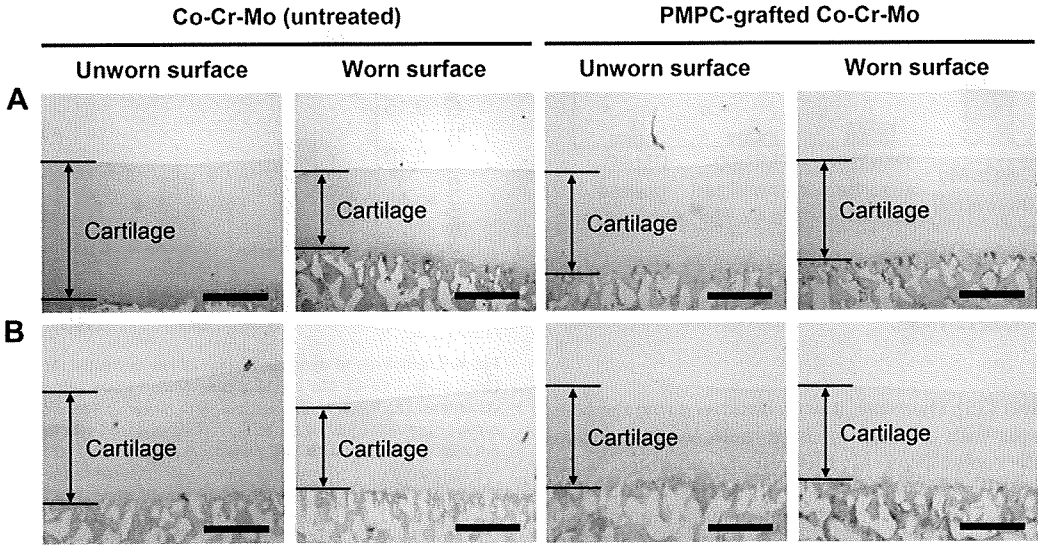

Fig. 8. Histological findings of the articular cartilage pins after 5×10^3 cycles of friction tests. (A) H&E stained, and (B) safranin-O stained. Bar; 500 μm.

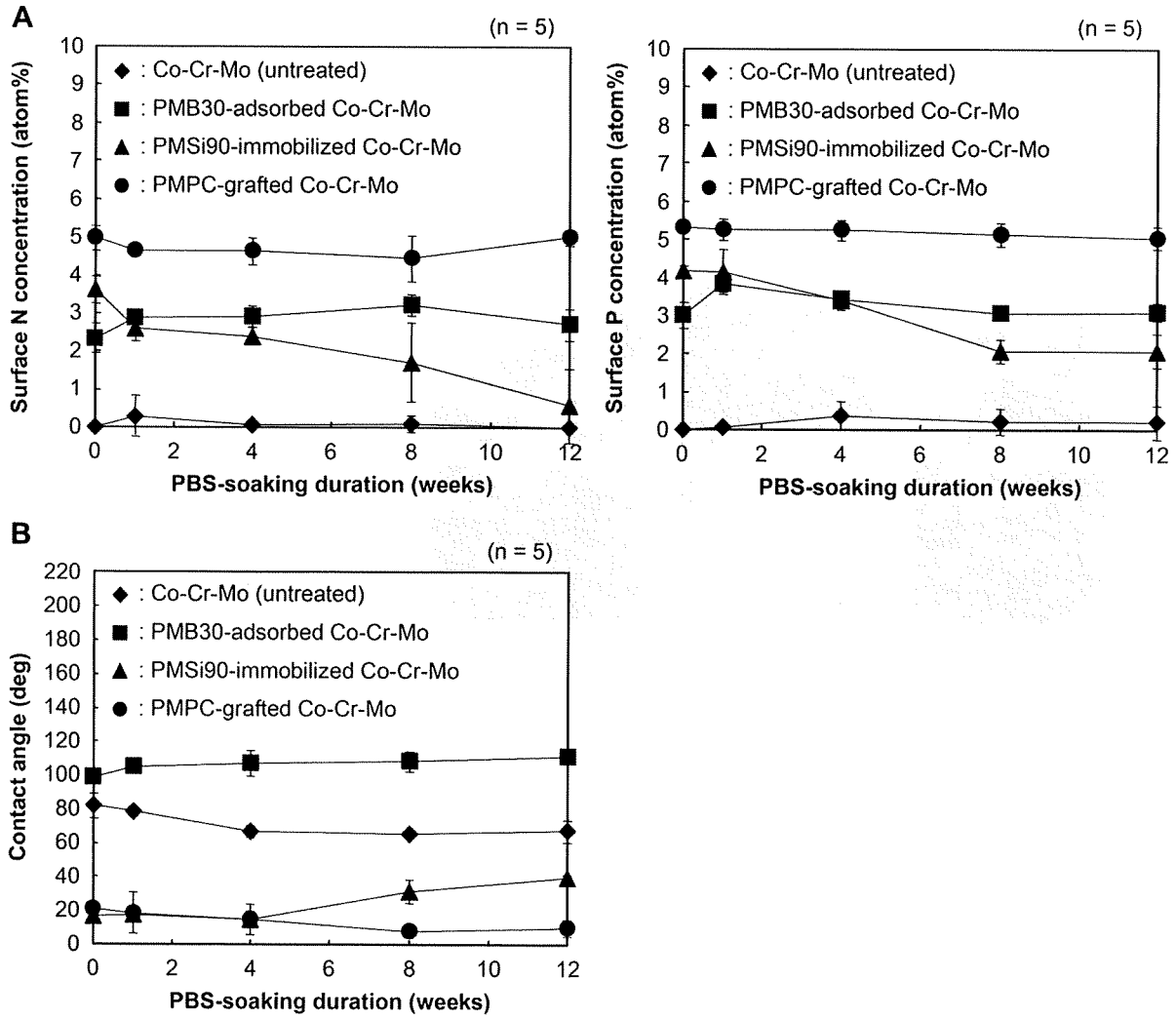

Fig. 9. Time course of the surface-modification layer of the untreated, MPC polymer-coated and PMPC-grafted Co–Cr–Mo during PBS soaking with 120 rpm shaking at 37 °C. (A) Surface N and P concentrations by XPS, and (B) static-water contact angle. Bar: Standard deviations.

[27,28]. In this study, it was found that the cartilage/PMPC-grafted Co–Cr–Mo interface mimicking a natural joint showed low friction (friction coefficient was <0.01), i.e., as low as that of cartilage/cartilage interface. Hence, it was considered that the PMPC-grafted Co–Cr–Mo surface is well suited for application on the artificial femoral head that would chafe against articulating cartilage. We expect that hemi-arthroplasty with a PMPC-grafted Co–Cr–Mo femoral head will be a promising option that preserves acetabular cartilage and extends the duration before total hip arthroplasty (THA) in young patients. Moreover, we consider that these effects would occur continuously. In Fig. 7B, the friction coefficient shows a test duration-dependent response for articular cartilage against the untreated Co–Cr–Mo sample due to the continued loading of the cartilage tissue and the ensuing loss of fluid-film formation (or rehydration). It was thought that the thickness of the cartilage tissue atrophied due to the fairly poor access of the cartilage tissue to water (Fig. 8). Decreased water content often leads to the degradation of cartilage function. Although cartilage tissues are able to produce matrix components throughout life, i.e., carry out regeneration, their production cannot keep pace with the repair requirements after acute damage to articular cartilage; such damages limit the longevity of the artificial femoral head and its stability after hemi-arthroplasty. In contrast, in articular cartilage against the PMPC-grafted Co–Cr–Mo sample, the friction coefficient remained at a steady low value due to the rehydration of the continuously loaded cartilage tissue, and the articular cartilage surface was preserved.

In Fig. 6A, the PMB30-adsorbed and PMSi90-immobilized Co–Cr–Mo samples show a slightly higher friction coefficient than the untreated Co–Cr–Mo sample in water at room temperature. Some pores in the PMB30 and PMSi90 layers on the Co–Cr–Mo surface could be observed (Fig. 3); these may have occurred due to the low density of the material because physical adsorption or chemical immobilization of the polymer was used as the surface modification method. Therefore, it is assumed that a sliding couple with cartilage and low-density MPC polymer layer may cause high friction by stick-slip motion with interpenetration [18]. Furthermore, the MPC polymer-coated Co–Cr–Mo showed a lower friction coefficient than the untreated Co–Cr–Mo in BS mixture at 37 °C (Fig. 6B). It was thought that the interpenetration of cartilage and low-density MPC polymer layer was blocked by the protein of BS presented between the interfaces. In contrast, the friction coefficient of the PMPC-grafted Co–Cr–Mo sample was drastically as compared with that of the untreated Co–Cr–Mo sample; the degree

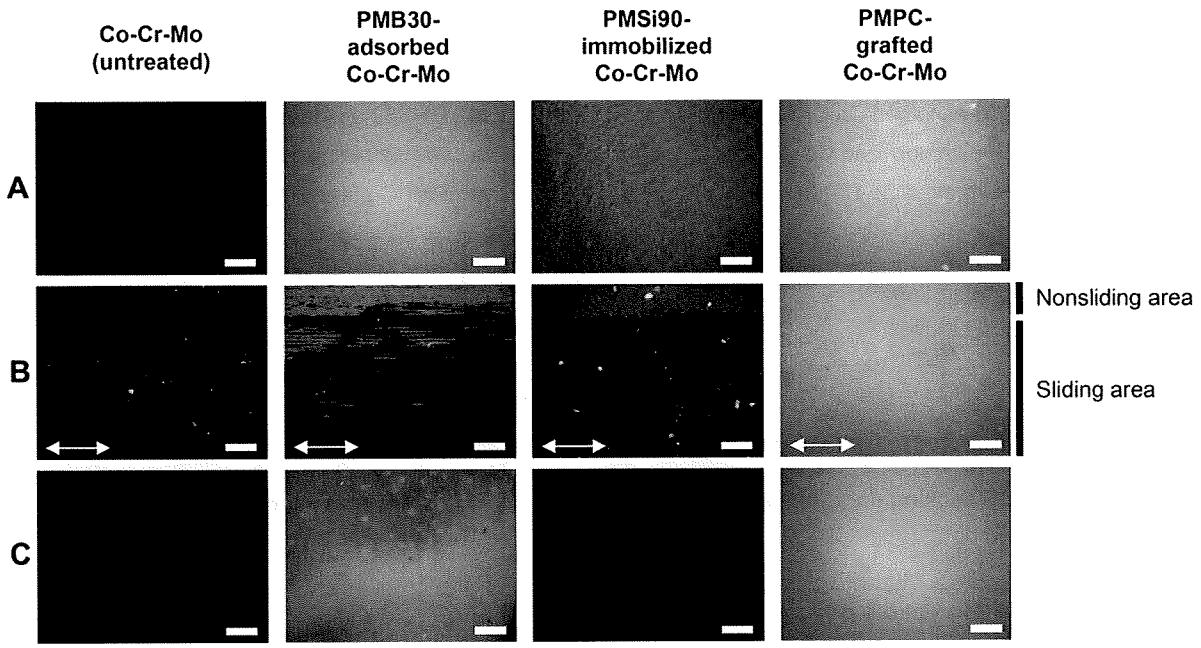

Fig. 10. FM images of the untreated Co–Cr–Mo, MPC polymer-coated Co–Cr–Mo, and PMPC-grafted Co–Cr–Mo surfaces. FM images of the surface before tests (A), after 100 cycles of friction tests with BS lubricant (B), and after 12 weeks of PBS-soaking tests (C). Bar; 200 μm. Arrow; Sliding direction of friction test.

of reduction in the coefficient was 93%. PMPC-grafted Co–Cr–Mo might have a high density because the polymerization method used was surface-initiated graft polymerization, termed as the "grafting from" method [19,29]. A sliding couple with cartilage tissue and high-density PMPC layer fabricated by the "grafting from" method may be responsible for low friction, such as that in the case of "super-lubricity," because of resistance to interpenetration by volume effects resulting from the mobility of hydrophilic macromolecules of cartilage tissue and the PMPC-grafted layer [30–32].

As shown in Fig. 7A, the friction coefficients of the articular cartilage against the untreated and PMPC-grafted Co–Cr–Mo samples decreased with an increasing load in the initial 10 cycles. The elastic articular cartilage tissue and PMPC-grafted layer was slightly deformed by the loads; the low friction coefficient might occur in order to increase the contact area of the fluid film's concave surface. However, the friction coefficient of the articular cartilage against the untreated Co–Cr–Mo at 100 cycles decreased to 0.082 up to loads of 1.96 N; a further increase in loads up to 9.8 N resulted in elevated friction coefficients. Under a high load, water exudes slowly from the articular cartilage with sliding [27]. As the result of water loss, the thickness of the surface layer and/or fluid film reduces, and the water content of the surface-hydration layer decreases. Consequently, the degree of adhesion of articular cartilage to the Co–Cr–Mo surface increases due to a lack of rehydration and because of the increase in frictional force. In contrast, the PMPC-grafted Co–Cr–Mo sample at 100 cycles showed a remarkably low friction coefficient that reached approximately <0.010 at a load of 9.80 N. We consider that this result implies that the rehydration and hydrodynamic lubrication mechanism of the articular cartilage is supported by the hydrated PMPC-grafted layer, similar to the interface between cartilage/cartilage of the natural joint.

The friction coefficients of cartilage/untreated Co–Cr–Mo interface with all MPC polymer-containing BS mixtures as a lubricant were drastically lower as compared with that with the non-additive BS mixture (Fig. 6C). Synovial fluid as a whole, and all its components such as hyaluronic acid, glycoprotein (mainly lubricin), and surface-active phospholipids, have been proposed as lubricants responsible for boundary lubrication in the natural joint [33]. Similarly, it is considered that the additives of MPC polymer would play the role akin to synovial phospholipids for boundary lubrication, and the adsorption of the MPC polymer to the sliding surface could prevent direct contact between the cartilage and the untreated Co–Cr–Mo and hence decrease the frictional force between them. However, in the case of additives, the lubricity may change depending on the ambient *in vitro* and *in vivo* conditions, because the additives probably diffuse to synovial fluid *in vivo*.

The amounts of the representative protein, BSA, γ-globulins, and fibrinogen, adsorbed on the modified Co–Cr–Mo surface with the MPC polymer were significantly low, these reached to 7%–50% of that of the untreated surface, as shown in Fig. 5. It is hypothesized that the mechanism underlying protein adsorption resistivity of a surface modified by the MPC polymer is based on the water structure resulting from the interactions between water molecules and phosphorylcholine groups [34]. The large amount of free water around the phosphorylcholine group is considered to detach proteins easily and prevent conformational changes in the adsorbed proteins even when the proteins attached to the surface [3,34]. The reduction in protein adsorption is also considered to be caused by the presence of a hydrated layer around the phosphorylcholine group [35]. The latter consideration is consistent with the results of the water contact angle measurement, friction test, and TEM and FM observations of the Co–Cr–Mo samples whose surfaces were modified by the MPC polymer. It should be noted that the porous structure (low density) of the PMB30-adsorption and PMSi90-immobilization layer (in dry conditions) hardly affected the protein adsorption. Therefore, the Co–Cr–Mo sample whose surface is modified by the MPC polymer is expected to exhibit tissue and blood compatibility, i.e., biocompatibility, because previous studies have reported that the MPC polymer-modified surfaces exhibit *in vivo* biocompatibility [6–16].

5. Conclusions

In this study, we systematically investigated the surface properties of the various surface modification layers formed on the Co–Cr–Mo surface by the MPC polymer by dip coating or photoinduced radical grafting. We conclude that several important issues are involved in the long-term retention of the benefits of the MPC polymer used in artificial joints under variable and multidirectional loads, for example, strong bonding between the MPC polymer and the Co–Cr–Mo surface as also a high density of the MPC polymer. We suggest that the MPSi intermediate layer and photoinduced radical graft polymerization should be employed to create strong covalent bonding between the surface modification layer and Co–Cr–Mo substrate and to retain the high density of the polymer chains of that layer. The cartilage/PMPC-grafted Co–Cr–Mo interface, which mimicked a natural joint, showed an extremely low friction coefficient of <0.01, a value as low as that of a natural cartilage interface. We expect that the PMPC-grafted Co–Cr–Mo femoral head for hemi-arthroplasty will be a promising option for preserving acetabular cartilage and extending the duration before THA.

Acknowledgements

This study was supported by the Health and Welfare Research Grant for Translational Research (H17-005), Research on Medical Devices for Improving Impaired QOL (H20-004) from the Japanese Ministry of Health, Labour and Welfare. We thank Mr. Y. Yoshihara and Ms. Y. Nakao, Japan Medical Materials Corporation, for their excellent technical assistance.

Appendix

Figures with essential colour discrimination. Certain figures in this article, in particular Figures 8 and 10, are difficult to interpret in black and white. The full colour images can be found in the on-line version, at doi:10.1016/j.biomaterials.2009.09.083.

References

[1] Healy WL, Lemos DW, Appleby D, Lucchesi CA, Saleh KJ. Displaced femoral neck fractures in the elderly: outcomes and cost effectiveness. Clin Orthop Relat Res 2001;383:229–42.
[2] Beaulé PE, Amstutz HC, Le Duff M, Dorey F. Surface arthroplasty for osteonecrosis of the hip: hemiresurfacing versus metal-on-metal hybrid resurfacing. J Arthroplasty 2004;19(8 Suppl. 3):54–8.
[3] Kyomoto M, Moro T, Miyaji F, Hashimoto M, Kawaguchi H, Takatori Y, et al. Effects of mobility/immobility of surface modification by 2-methacryloyloxyethyl phosphorylcholine polymer on the durability of polyethylene for artificial joints. J Biomed Mater Res A 2009;90(2):362–71.
[4] Kyomoto M, Moro T, Miyaji F, Hashimoto M, Kawaguchi H, Takatori Y, et al. Effect of 2-methacryloyloxyethyl phosphorylcholine concentration on photo-induced graft polymerization of polyethylene in reducing the wear of orthopaedic bearing surface. J Biomed Mater Res A 2008;86(2):439–47.
[5] Kyomoto M, Moro T, Miyaji F, Konno T, Hashimoto M, Kawaguchi H, et al. Enhanced wear resistance of orthopedic bearing due to the cross-linking of poly(MPC) graft chains induced by gamma-ray irradiation. J Biomed Mater Res B Appl Biomater 2008;84(2):320–7.
[6] Moro T, Takatori Y, Ishihara K, Konno T, Takigawa Y, Matsushita T, et al. Surface grafting of artificial joints with a biocompatible polymer for preventing periprosthetic osteolysis. Nature Mater 2004;3:829–37.
[7] Moro T, Takatori Y, Ishihara K, Nakamura K, Kawaguchi H. 2006 Frank Stinchfield Award: grafting of biocompatible polymer for longevity of artificial hip joints. Clin Orthop Relat Res 2006;453:58–63.
[8] Moro T, Kawaguchi H, Ishihara K, Kyomoto M, Karita T, Ito H, et al. Wear resistance of artificial hip joints with poly(2-methacryloyloxyethyl phosphorylcholine) grafted polyethylene: comparisons with the effect of polyethylene cross-linking and ceramic femoral heads. Biomaterials 2009;30(16):2995–3001.
[9] Kyomoto M, Ishihara K. Self-initiated surface graft polymerization of 2-methacryloyloxyethyl phosphorylcholine on poly(ether–ether–ketone) by photo-irradiation. ACS Appl Mater Interfaces 2009;1(3):537–42.
[10] Sibarani J, Takai M, Ishihara K. Surface modification on microfluidic devices with 2-methacryloyloxyethyl phosphorylcholine polymers for reducing unfavorable protein adsorption. Colloids Surf B Biointerfaces 2007;54(1):88–93.
[11] Ueda T, Oshida H, Kurita K, Ishihara K, Nakabayashi N. Preparation of 2-methacryloyloxyethyl phosphorylcholine copolymers with alkyl methacrylates and their blood compatibility. Polym J 1992;24(11):1259–69.
[12] Konno T, Ishihara K. Temporal and spatially controllable cell encapsulation using a water-soluble phospholipid polymer with phenylboronic acid moiety. Biomaterials 2007;28(10):1770–7.
[13] Xu Y, Takai M, Konno T, Ishihara K. Microfluidic flow control on charged phospholipid polymer interface. Lab Chip 2007;7(2):199–206.
[14] Snyder TA, Tsukui H, Kihara S, Akimoto T, Litwak KN, Kameneva MV, et al. Preclinical biocompatibility assessment of the EVAHEART ventricular assist device: coating comparison and platelet activation. J Biomed Mater Res A 2007;81(1):85–92.
[15] Ueda H, Watanabe J, Konno T, Takai M, Saito A, Ishihara K. Asymmetrically functional surface properties on biocompatible phospholipid polymer membrane for bioartificial kidney. J Biomed Mater Res A 2006;77(1):19–27.
[16] Kyomoto M, Moro T, Konno T, Takadama H, Yamawaki N, Kawaguchi H, et al. Enhanced wear resistance of modified cross-linked polyethylene by grafting with poly(2-methacryloyloxyethyl phosphorylcholine). J Biomed Mater Res A 2007;82(1):10–7.
[17] Ishihara K, Ueda T, Nakabayashi N. Preparation of phospholipid polymers and their properties as polymer hydrogel membranes. Polym J 1990;22(5):355–60.
[18] Kyomoto M, Iwasaki Y, Moro T, Konno T, Miyaji F, Kawaguchi H, et al. High lubricious surface of cobalt–chromium–molybdenum alloy prepared by grafting poly(2-methacryloyloxyethyl phosphorylcholine). Biomaterials 2007;28(20):3121–30.
[19] Kyomoto, M., Moro, T., Iwasaki, Y., Miyaji, F., Kawaguchi, H., Takatori, Y., et al. Superlubricious surface mimicking articular cartilage by grafting poly(2-methacryloyloxyethyl phosphorylcholine) on orthopaedic metal bearings. J Biomed Mater Res A, in press.
[20] Wang JH, Bartlett JD, Dunn AC, Small S, Willis SL, Driver MJ, et al. The use of rhodamine 6G and fluorescence microscopy in the evaluation of phospholipid-based polymeric biomaterials. J Microsc 2005;217(Pt 3):216–24.
[21] Arendt SA, Bailey SJ, editors. ASTM F732-00: standard test method for wear testing of polymeric materials used in total joint prostheses. Annual book of ASTM standards, vol. 13; 2004.
[22] Kyomoto M, Moro T, Konno T, Takadama H, Kawaguchi H, Takatori Y, et al. Effects of photo-induced graft polymerization of 2-methacryloyloxyethyl phosphorylcholine on physical properties of cross-linked polyethylene in artificial hip joints. J Mater Sci Mater Med 2007;18:1809–15.
[23] Yoshida K, Greener EH. Effects of coupling agents on mechanical properties of metal oxide-polymethacrylate composites. J Dent 1994;22:57–62.
[24] Matinlinna JP, Vallittu PK. Bonding of resin composites to etchable ceramic surfaces – an insight review of the chemical aspects on surface conditioning. J Oral Rehabil 2007;34(8):622–30.
[25] Zhang Z, Berns AE, Willbold S, Buitenhuis J. Synthesis of poly(ethylene glycol) (PEG)-grafted colloidal silica particles with improved stability in aqueous solvents. J Colloid Interface Sci 2007;310(2):446–55.
[26] Ishikawa Y, Hiratsuka K, Sasada T. Role of water in the lubrication of hydrogel. Wear 2006;261:500–4.
[27] Katta J, Jin Z, Ingham E, Fisher J. Biotribology of articular cartilage – a review of the recent advances. Med Eng Phys 2008;30(10):1349–63.
[28] Bell CJ, Ingham E, Fisher J. Influence of hyaluronic acid on the time-dependent friction response of articular cartilage under different conditions. Proc Inst Mech Eng [H] 2006;220(1):23–31.
[29] Matsuda T, Kaneko M, Ge S. Quasi-living surface graft polymerization with phosphorylcholine group(s) at the terminal end. Biomaterials 2003;24:4507–15.
[30] Raviv U, Glasson S, Kampf N, Gohy JF, Jérôme R, Klein J. Lubrication by charged polymers. Nature 2003;425:163–5.
[31] Chen M, Briscoe WH, Armes SP, Klein J. Lubrication at physiological pressures by polyzwitterionic brushes. Science 2009;323(5922):1698–701.
[32] Kobayashi M, Terayama Y, Hosaka N, Kaido M, Suzuki A, Yamada N, et al. Friction behavior of high-density poly(2-methacryloyloxyethyl phosphorylcholine) brush in aqueous media. Soft Matter 2007;2:740–6.
[33] Sawae Y, Yamamoto A, Murakami T. Influence of protein and lipid concentration of the test lubricant on the wear of ultra high molecular weight polyethylene. Tribol Int 2008;41(7):648–56.
[34] Goda T, Konno T, Takai M, Ishihara K. Photoinduced phospholipid polymer grafting on Parylene film: advanced lubrication and antibiofouling properties. Colloids Surf B Biointerfaces 2007;54(1):67–73.
[35] Hoshi T, Sawaguchi T, Konno T, Takai M, Ishihara K. Preparation of molecular dispersed polymer blend composed of polyethylene and poly(vinyl acetate) by in situ polymerization of vinyl acetate using supercritical carbon dioxide. Polymer 2007;48(6):1573–80.

Selection of highly osteogenic and chondrogenic cells from bone marrow stromal cells in biocompatible polymer-coated plates

G. Liu,[1,2] K. Iwata,[1,2] T. Ogasawara,[1,2] J. Watanabe,[3] K. Fukazawa,[3] K. Ishihara,[3,4] Y. Asawa,[1] Y. Fujihara,[1] U.-L. Chung,[4] T. Moro,[5] Y. Takatori,[2] T. Takato,[2] K. Nakamura,[2] H. Kawaguchi,[2] K. Hoshi[1]

[1]*Department of Cartilage and Bone Regeneration (Fujisoft), Graduate School of Medicine, The University of Tokyo, Tokyo, Japan*

[2]*Department of Sensory and Motor System Medicine, Graduate School of Medicine, The University of Tokyo, Tokyo, Japan*

[3]*Department of Materials Engineering, School of Engineering, The University of Tokyo, Tokyo, Japan*

[4]*Deparment of Bioengineering, School of Engineering, The University of Tokyo, Tokyo, Japan*

[5]*Center of Disease Biology and Integrative Medicine, Graduate School of Medicine, The University of Tokyo, Tokyo, Japan*

Received 4 September 2007; revised 31 October 2008; accepted 21 November 2008
Published online 27 March 2009 in Wiley InterScience (www.interscience.wiley.com). DOI: 10.1002/jbm.a.32460

Abstract: To enrich the subpopulation that preserves self-renewal and multipotentiality from conventionally prepared bone marrow stromal cells (MSCs), we attempted to use 2-methacryloyloxyethyl phosphorylcholine (MPC) polymer-coated plates that selected the MSCs with strong adhesion ability and evaluated the proliferation ability or osteogenic/chondrogenic potential of the MPC polymer-selected MSCs. The number of MSCs that were attached to the MPC polymer-coated plates decreased with an increase in the density of MPC unit (0–10%), whereas no significant difference in the proliferation ability was seen among these cells. The surface epitopes of CD29, CD44, CD105, and CD166, and not CD34 or CD45, were detectable in the cells of all MPC polymer-coated plates, implying that they belong to the MSC category. In the osteogenic and chondrogenic induction, the MSCs selected by the 2–5% MPC unit composition showed higher expression levels of osteoblastic and chondrocytic markers (COL1A1/ALP, or COL2A1/COL10A1/Sox9) at passage 2, compared with those of 0–1% or even 10% MPC unit composition, while the enhanced effects continued by passage 5. The selection based on the adequate cell adhesiveness by the MPC polymer-coated plates could improve the osteogenic and chondrogenic potential of MSCs, which would provide cell sources that can be used to treat the more severe and various bone/cartilage diseases. © 2009 Wiley Periodicals, Inc. J Biomed Mater Res 92A: 1273–1282, 2010

Key words: bone marrow stromal cell (MSC); 2-methacryloyloxyethyl phosphorylcholine (MPC) polymer; osteogenesis; chondrogenesis; cell adhesion

INTRODUCTION

Bone marrow mesenchymal stem cells or stromal cells (MSCs) retain the potential to differentiate into multiple cell lineages that include osteoblasts, chondrocytes, adipocytes, myoblasts, and early progenitors of neural cells.[1–3] Because MSCs can be easily obtained from a small aspirate of bone marrow and they rapidly proliferate during the early passages of the expansion culture, human MSCs are regarded as one of the attractive cell sources for regenerative medicine in bone, cartilage, heart, nerve, and other tissues. However, MSCs are principally collected from bone marrow aspirates only through their selection by adhesiveness onto the plastic culture dishes,[4] and therefore, they include various subpopulations of cells which possess different proliferation rates or differentiation potentials. During the long-term culture with repeated passages, the balance among the subpopulations in the MSCs changes as a result of the difference in the proliferation rates, which may cause a deterioration of the self-renewal property or multipotentiality after repeated passages.[5]

To isolate or enrich the subpopulation that preserves the self-renewal and the multipotentiality

Correspondence to: K. Hoshi; e-mail: pochi-tky@umin.net
Contract grant sponsor: Grants-in-Aid for Scientific Research from the Japanese Ministry of Education, Culture, Sports, Science and Technology, Japan; contract grant numbers: 18659593, 18592166

© 2009 Wiley Periodicals, Inc.

from the conventionally prepared MSCs, various kinds of efforts have been made in the past decade. It was reported that the sizes and structures of the cells could distinguish the cells possessing a great potential for multilineage differentiation, termed rapid self-renewal (RS) cells, from the heterogeneity of the MSCs.[6] The RS cells had a shaped round shape with approximately a 7-μm diameter, and could be purified by using a 10-μm filter.[6] However, some limitations had been pointed out in the paper that the filtration process could only provide a low yield of purified RS cells because the other-sized cells rapidly obstructed the filter pores. The RS cells were also characterized by the low forward scatter and low side scatter of light during a flow cytometric analysis.[7] During cell sorting with the criteria of a low forward scatter and low side scatter, the subpopulation was successfully enriched for the RS cells, which increased the differentiation potential for osteoblasts and adipocytes. Although the cell sorting technologies of flow cytometry have been highly anticipated for the effective isolation of a specific subpopulation, some issues including the acquisition rates of target cells, the prevention of pathogen contamination, or the mechanical and thermodynamic damage to cells by the cell sorter should be cautiously evaluated before clinical use.

The MSC isolation was also attempted, using some surface epitopes, including CD13, CD29 (integrin β1), CD44 (hyaluronan receptor), CD73(SH3), CD90 (Thy-1), CD105 (Endoglin), CD166 (activated leukocyte cell adhesion molecule/ALCAM), PDGF receptor or Stro-1, all of which are highly expressed in the MSCs.[6,8] The combination with CD34 and CD45 (leukocyte common antigen/LCA), either of which is a marker of hematopoietic stem cells, could exclude the hematopoietic lineage from the MSCs. However, as the expression level of the markers in the MSCs was quite similar to those of fibroblastic cells that are also contained in bone marrow aspirates and that decrease the multipotency and self-renewal,[8] specific selection of the MSCs from such heterogenetic cell populations could not be sufficiently obtained even by flow cytometry or a magnetic cell sorting system.

Serum deprivation is one of the possible methods to concentrate the subpopulation possessing a high proliferation and differentiation potential from the heterogeneity of the MSCs.[9] When early-passage human MSCs were cultured in serum-free medium without cytokines or other supplements, a subpopulation of the cells was attached to the plates and survived for 2–4 weeks. Afterward, such cells began to proliferate in serum-containing medium, and prominently showed stem cell properties including long telomeres or a high expression of the octomer-binding transcription factor 4 (OCT-4). The findings suggested that such cells that possess a strong adherent ability and survive despite the harsh environments may show a high quality of stem cell properties.

On the basis of this hypothesis, we attempted to select some subpopulations of MSCs showing a high adhesiveness on the culture plates. For selection, the cell adhesiveness was adjusted by the coating of 2-methacryloyloxyethyl phosphorylcholine (MPC) polymers. The MPC polymers are designed with inspiration from cell membrane surface and well-known biocompatible polymers that can reduce protein adsorption or subsequent cell adhesion significantly.[10–12] On the basis of this fundamental biocompatibility, the MPC polymers have been used for preparing medical devices, for example, the surfaces of intravascular stents, intravascular guide wires, soft contact lenses, an artificial lung or artificial hip joint.[13–16] Some of these are already clinically available.

We examined the selectivity of MSCs using MPC polymer-coated plates and evaluated the proliferation ability or differentiation potential of the MPC polymer-selected subpopulation. Especially, we focused on the osteogenic and chondrogenic ability, because bone and cartilage tissue engineering using MSCs are highly desired for clinical applications.

MATERIALS AND METHODS

Preparation of MPC polymer-coated plates

Coating of the MPC polymer onto the polystyrene (PS) surface of the culture plates was performed by a simple dip-coating using MPC polymer solutions. The composition of MPC units was controlled by mixing poly(*n*-butyl methacrylate) (Poly(BMA)) and poly(MPC-*co*-BMA)(PMB30). These polymers were synthesized by a conventional radical polymerization. Poly(BMA) was a homopolymer of BMA without MPC unit (molecular weight = 4.0×10^5), and PMB30 was a copolymer composed of 30% of MPC units and 70% of BMA units (molecular weight = 6.0×10^5). In this study, each polymer was dissolved in a mixture of tetrahydrofran (THF) and ethanol (1:9 by volume) as solvents, and then poly(BMA) and PMB30 solutions were prepared (0.25 wt %). To control the MPC unit composition in the range between 0, 1, 2, 5, and 10% of MPC unit composition, these polymer mixtures in the solution were prepared. The dip-coating was carried out in the clean bench as follows: (i) 200 μL of the solution was poured into the each culture plates (ϕ 2.2 cm), (ii) the polymer solution was removed after 5 s, (iii) the coating was repeated and the resulting culture plate was dried over night, and (iv) the MPC polymer-coated culture plate was sterilized by UV irradiation for an adequate time. Therefore, the resulting MPC unit density on the plate was 0, 1, 2, 5, and 10% MPC unit composition.

Surface elemental analysis of the MPC polymer-coated PS plate was carried out by X-ray photoelectron spectroscopy (XPS, AXIS-His, Shimadzu/KRATOS, Kyoto, Japan). The X-ray source used for XPS measurements was Mg Ka source. The take-off angle of the photoelectrons was fixed

as 90°. At least five points of the sample were measured by XPS and these intensities were averaged before the following calculation. The surface compositions of the MPC units were calculated as follows. The ratio of signal intensity at 133 eV based on the phosphorus atom attributed to the MPC units over that at 285 eV based on the carbon atoms attributed methyl groups and methylene groups in both BMA and MPC units was determined. The calibration was carried out using the ratio obtained from the XPS spectra of both poly(BMA) and poly(MPC)-coated PS plate as 0% and 100% of MPC unit, respectively.

MSC preparation and selection by MPC polymer-coated plates

All procedures for the present experiments were approved by the ethics committee or institutional committee for animal research of the University of Tokyo Hospital (ethics permission #622). Figure 1(a) indicates the experimental design. Human MSCs were obtained from the femur of osteoarthritic patients who underwent total hip replacement at the University of Tokyo Hospital, after informed consent. Cells in bone marrow aspirates (100 μL/φ 2.2 cm dish) were seeded on MPC polymer-coated culture plates with various MPC unit compositions as 0–10%, and cultured using the hMSC bullet kit (Cambrex, East Ruatherford, NJ) in a 37°C/5% CO_2 incubator. Rat MSCs were collected from 6-week-old male Sprague-Dawley rats (Nisseizai, Tokyo, Japan). After the epiphyses of the tibias were removed, the marrow was flushed out by using a syringe filled with medium and filtered through a 70-μm nylon mesh. The obtained bone marrow materials (100 μL/φ 2.2 cm dish) were plated and cultured in the same manner as human MSCs.

The cells were harvested by treatment using trypsin-EDTA solution. After the cell harvest of the primary culture from the MPC polymer-coated plates, the cells were reseeded onto the conventional PS culture plates at a density of 5.0×10^3 cells/cm^2. Passages were performed when the cells were approaching confluence. The medium was changed three times per week. The cell numbers were counted by a haematocytometer, while the viability of the cells was checked by trypan blue staining. Cell proliferation was also colorimetrically measured by cell counting kit-8 (Dojin, Kumamoto, Japan), a week after cell seeding.

Flow cytometric analysis

Cells were harvested using trypsin-EDTA solution, centrifuged at 1500*g* for 5 min, and resuspended at 5×10^6 cells/mL in phosphate-buffered saline (PBS) containing 3% fetal bovine serum. Aliquots containing 10^5 cells were incubated with individual primary antibodies or control IgG for 30 min at room temperature. The cells were washed in PBS containing 3% fetal bovine serum and incubated with a fluorescent conjugated secondary antibody for 30 min at room temperature. Samples were analyzed using a FACS LSL II (BD, Franklin Lakes, NJ). The following monoclonal antibodies were used: mouse monoclonal antibodies against human CD29 (integrin β1, BD), human CD34 (Chemicon, Victoria, Australia), human CD44 (hyaluronan receptor, Ancell, Bayport, MN), human CD45 (LCA, Cymbus, Chandlers Ford, UK), human CD105 (Endoglin, Ancell), CD166 (ALCAM, Ancell), normal mouse IgG (Santa Cruz Biotechnology, Santa Cruz, CA) and fluorescein isothiocyanate (FITC)-conjugated rabbit antibody against mouse IgG (Santa Cruz Biotechnology).

Osteogenic and chondrogenic induction for MSCs

The osteogenic[1] or chondrogenic[17,18] differentiation was induced in MSCs according to previously reported procedures with some modifications. For the osteogenic differentiation, cells were seeded at 4.0×10^4 cells per 2.2-cm plates and maintained for 21 days in DMEM supplemented with 10% fetal bovine serum, 10 m*M* β-glycerophosphate, 100 n*M* Dexamethasone, and 50 μg/mL ascorbic acid-2-phosphate. For the chondrogenic differentiation, cells were seeded at 2×10^5 cells per 15 mL plastic centrifuge tube and maintained in 2 mL of serum-free a-MEM supplemented with 3500 μg/mL glucose, 6.25 μg/mL insulin, 6.25 μg/mL transferrin, 6.25 ng/mL selenite, 5.33 μg/mL linolate, 1.25 mg/mL bovine serum albumin, 10 ng/mL transforming growth factor-β3, 100 n*M* dexamethasone and 50 μg/mL ascorbic acid-2-phosphate. The cells were cultured under the chondrogenic status for 21 days. The medium was changed three times per week.

Total RNA extraction and real-time RT-PCR

The total RNA was isolated from MSC using the chaotropic Trizol method (Nippon-gene, Tokyo, Japan). The total mRNA (1 μg) was reverse transcribed using the Super Script reverse transcriptase with a random hexamer (Takara Shuzo, Shiga, Japan). The full-length or partial-length cDNA of the target genes, including the PCR amplicon sequences, was amplified by PCR, cloned into pCR-TOPO Zero II or pCR-TOPO II vectors (Invitrogen, Carlsbad, CA), and used as standard templates after linearization. The QuantiTect SYBR Green PCR Master Mix (Qiagen, Hilden, Germany) was used, and the SYBR Green PCR amplification and real-time fluorescence detection were performed with an ABI 7700 Sequence Detection system (Foster City, CA). All reactions were run in quadruplicate. The sequences of the primers were 5′-CTCCT CGCTTTCCTTCCTCT-3′ and 5′-GTGCTAAAGGTGCCAA TGGT-3′ for COL1A1; 5′-GAGTCAAGGGTGATCGTGGT-3′ and 5′-CACCTTGGTCT CCAGAAGGA-3′ for COL2A1; 5′-AGGAATGCCT GTGTCTGCT T -3′ and 5′-ACAGGCC TACCCAAACATGA-3′ for COL10A1; 5′- GACCCTTGACC CCCACAAT-3′ and 5′- GCTCGTACTGCATGTCCCCT-3′ for ALP; 5′-CATG AGCGAGGG CACTCC-3′ and 5′-TCGCTTCAGGTCAGCCTTG-3′ for Sox9; 5′-GAAGGTGA AGGTCGGAGTCA-3′ and 5′-GAAGATGGTGATGGGAT TTC-3′ for GAPDH.

Enzyme activity for ALP

The enzyme activity was histochemically detected in the MSCs in which the osteogenic differentiation was induced.

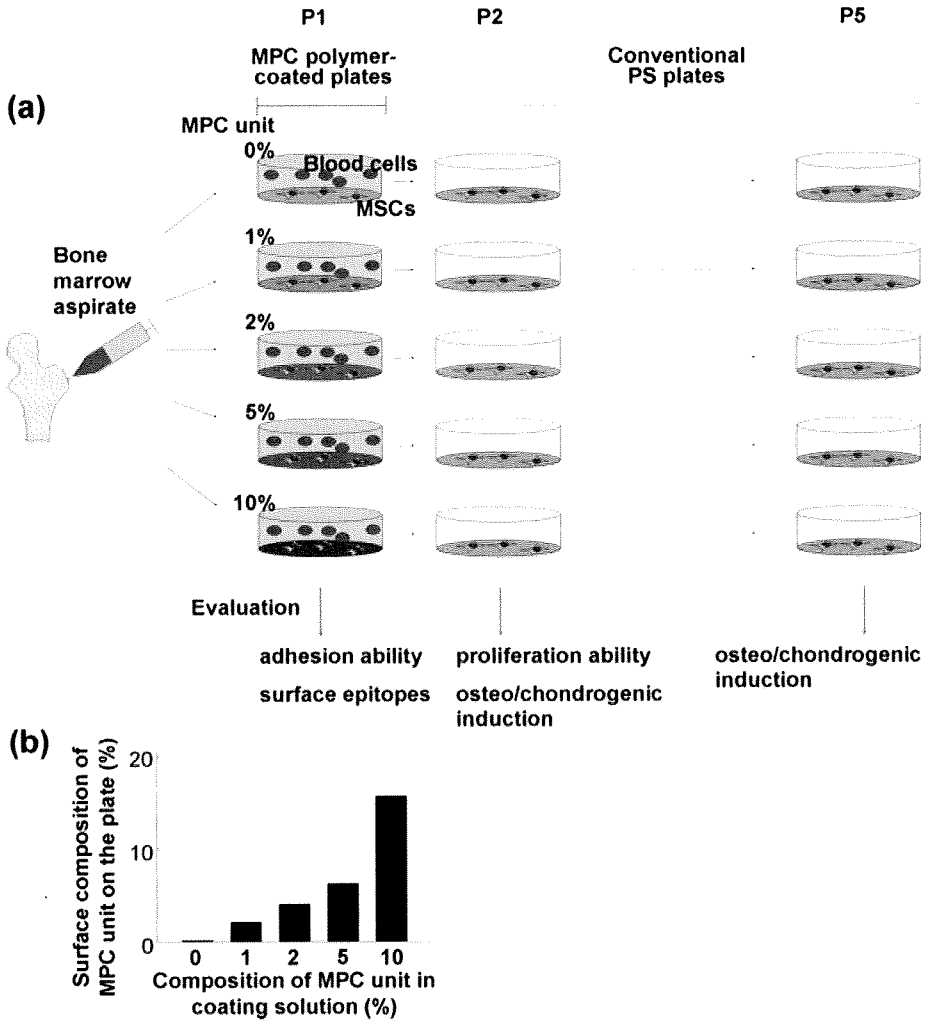

Figure 1. (a) The experimental design. Cells in bone marrow aspirates were seeded on MPC polymer-coated plates at the composition of 0–10% MPC unit, at passage 1, while the adhesion ability of MSCs to the MPC polymer-coated plates and the surface epitopes of MPC-selected cells were evaluated. Although cells were cultured on the MPC polymer-coated plates at passage 1, the cells were seeded onto the conventional PS plates thereafter. The proliferation of cells (passage 2) was measured by cell counting, while the differentiation potential for osteogenesis and chondrogenesis was examined at passages 2 and 5. (b) Relationship between MPC unit composition at the surface on PS plate after coating and that in polymer-coating solution. [Color figure can be viewed in the online issue, which is available at www.interscience.wiley.com.]

For ALP enzyme histochemistry, the cells were incubated with a mixture of 5 mg naphthol AS-BI phosphate (Sigma, St. Louis, MO) as a substrate and 18 mg of fast red violet LB salt (Sigma) diluted in 30 mL of 0.1 mol/L Tris-HCl buffer (pH 8.5). The images were taken by the digital camera, while the enzyme activity was quantitatively measured by histomorphometrical approaches using the software Scion Image alpha 4.0.3.2 (Scion, Frederick, MD).

RESULTS

Selection using MPC polymer-coated plates

Polymer coating of PS culture plate with the PMB30/poly(BMA) mixed solution was proceeded well, and the surface of the plate was covered with these polymers, completely. When the surface composition of MPC units on the plates was calculated from the XPS results, it was found that the MPC unit composition at the surface increased in parallel with that in the polymer mixed solution containing poly(BMA) and PMB30 used in a single dip coating as shown in Figure 1(b). We confirmed that the surface composition the MPC units could be controlled.

With these plates, we first selected some subpopulations of the MSCs according to the degrees of the adhesiveness on the culture plates coated with different compositions of the MPC unit. Human bone marrow aspirates (~0.1 mL) was seeded onto the culture plates with a 2.2 cm diameter coated with 0, 1, 2, 5, and 10%

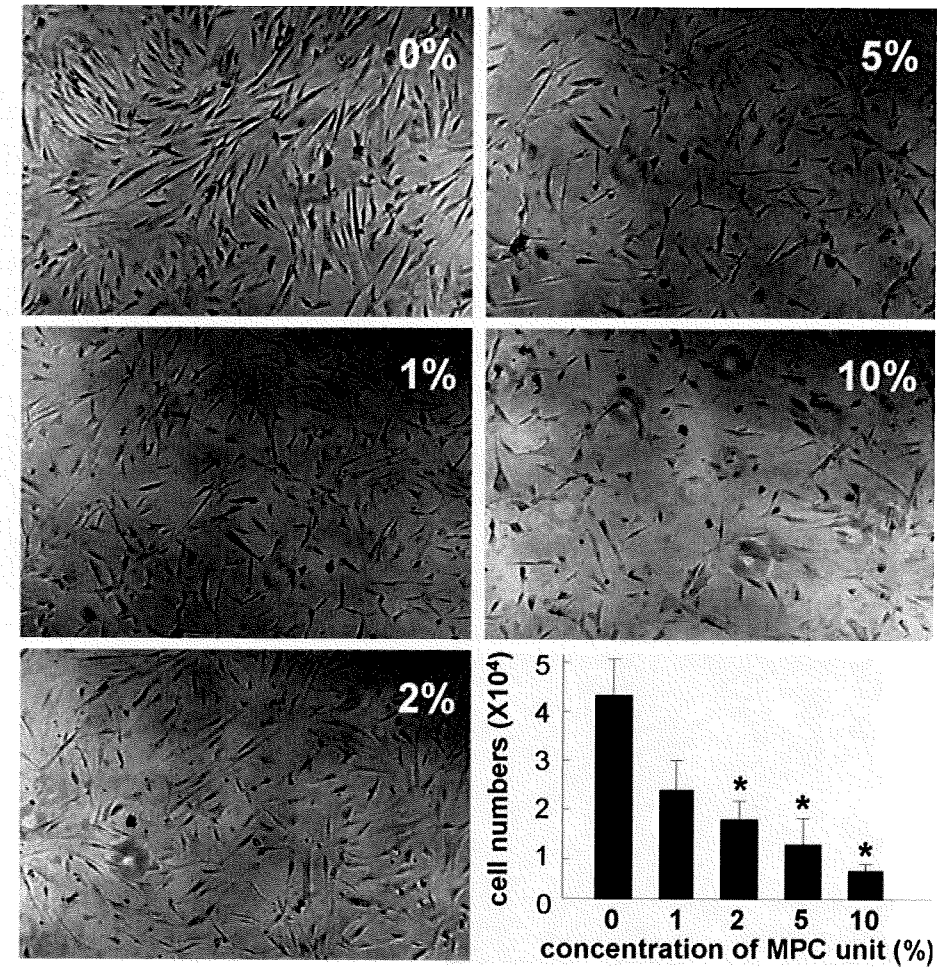

Figure 2. The adhesion of cells in human bone marrow aspirates onto the culture plates coated with MPC polymers with various compositions of MPC unit. The number of cells that were attached on the MPC polymer-coated plates at day 7 of the cell culture decreased according to the density of the MPC unit. All values are presented as mean plus standard deviation of five samples per group. Statistics were assessed using Dunnett's test (*$p < 0.01$ vs. 0% MPC unit composition).

MPC unit compositions. For 3 days, the number of adherent cells on the plate surface had plateaued on all plates. At 3 days, the medium was changed together with the floating cells and were replaced by another medium. The adherent cells continued to be cultured for four more days on the same MPC polymer-coated plates, and then were harvested for cell counting. The cells attached on the plate surface were observed to have a higher density on the dishes treated with a 0% MPC unit composition, compared with those of increasing the MPC unit composition, at 7 days (Fig. 2). The number of cells harvested from the plates had significantly decreased according to the increase in the density of the MPC polymer coating [Fig. 2 (graph)]. The cell numbers on the MPC polymer-coated dishes with 2% or 10% MPC units were approximately half or quarter of 0%, respectively.

To examine the proliferation ability of MPC polymer-selected MSCs, the cells harvested from each MPC polymer-coated plate were reseeded onto the conventional PS plates (φ 2.2 cm) with the same cell number of 1.9×10^4 in the second passage (passage 2), and then cultured for 7 days. The cells were equally proliferated during this period, while the total cell number after a 7 day-culture had not significantly changed among the cells derived from the different MPC polymer-coated plates [Fig. 3 (cell count)]. The result was represented by the experiment using the cell counting assay [Fig. 3 (cell counting assay)].

Surface epitopes of cells selected by MPC polymer-coated plates

We next examined the surface epitopes of the cells selected by the MPC polymer-coated plates (passage 1). It is known that CD29 (integrin β1), CD44 (hya-

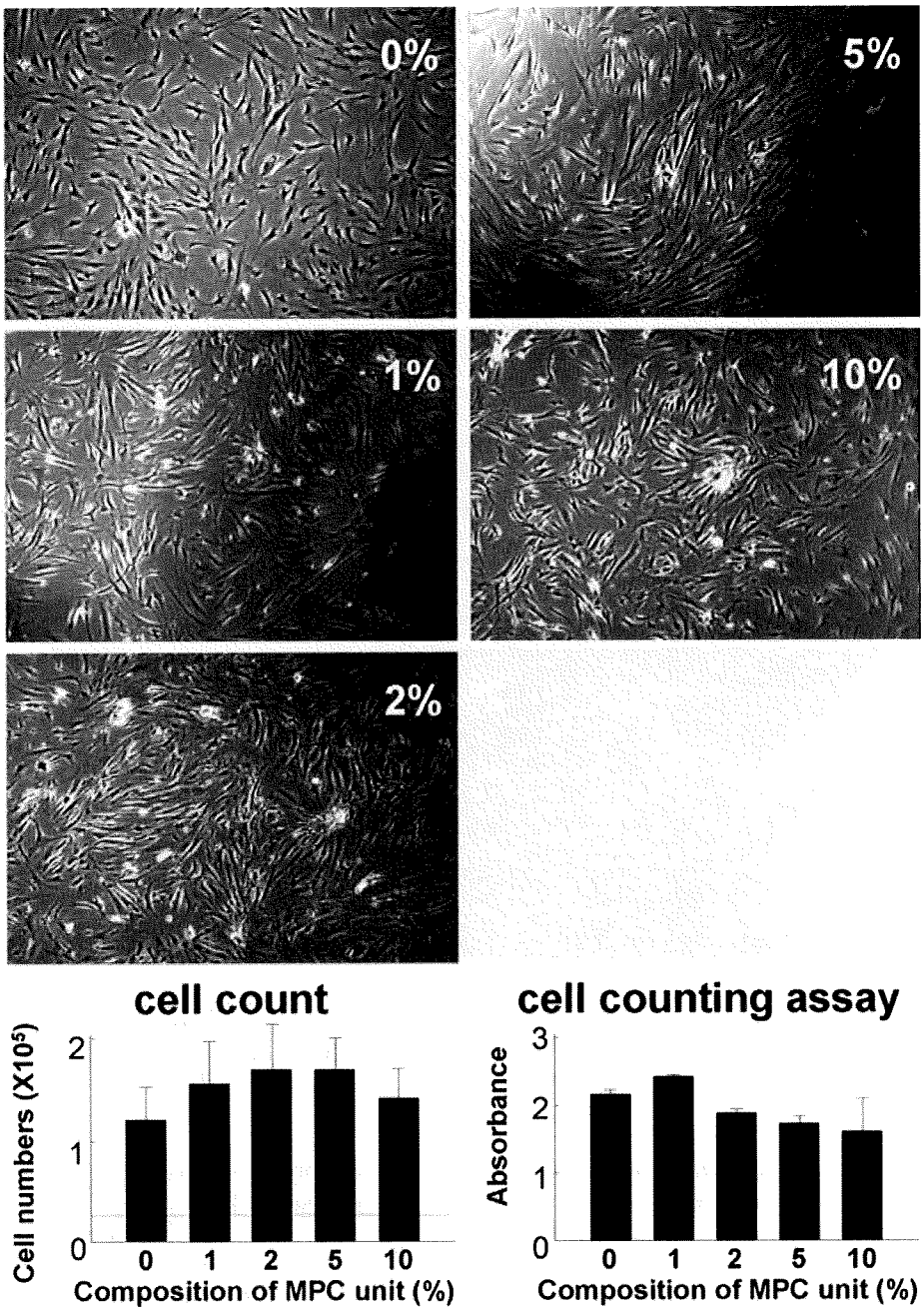

Figure 3. Proliferation of the cells that had been selected by the plate-coated MPC polymer with various MPC unit compositions. The cells cultured on the MPC polymer-coated plates were harvested and then reseeded onto the conventional PS plates. The numbers of human cells were counted at 7 days of culture (cell count). All values are presented as mean plus standard deviation of five samples per group. Statistics were assessed using Dunnett's test. No significant difference was seen among the proliferation of the cells harvested from each MPC polymer-coated plate (0–10% MPC unit composition). The dashed line indicats the number of cells originally seeded on the plate (1.9×10^3 cells). The result was represented by the experiment using the cell counting assay in the rat MSCs (cell counting assay). All values are presented as mean plus standard deviation of three measurements per group. No significant difference (Dunnett's test) was seen among each groups.

luronan receptor), CD105 (Endoglin) and CD166 (ALCAM) were expressed in MSC, but that CD34 and CD45 (LCA) were markers specific for heamatopoietic stem cells. Although the hematopoietic stem cell markers were negative in all cells selected by the plates coated with the 0, 1, 2, 5, or 10% of MPC unit

TABLE I
Expression of Surface Epitopes in MPC-Selected Cells

Surface Epitoptes	MPC 0%	MPC 1%	MPC 2%	MPC 5%	MPC 10%
CD29 (integrin β1)	++	++	+++	++	++
CD44 (Hyaluronan receptor)	++	++	++	++	++
CD105 (Endoglin)	+	+	+	+	+
CD166 (ALCAM)	+	+	+	+	+
CD34	−	−	−	−	−
CD45 (LCA)	−	−	−	−	−

composition, CD29, CD44, CD105, and CD166 were detectable in the cells of all MPC unit compositions. The levels of the MSC markers in the cells selected by the 1–10% MPC unit composition were almost similar to those in cells of 0% that corresponds to the control MSC, implying that the MPC polymer-selected cells belong to the category of MSC on the surface epitopes (Table I).

Osteogenic and chondrogenic potential of MPC polymer-selected cells

After the culture on the MPC polymer-coated plates (passage 1), the cells were cultured on the conventional PS culture plates for a long term with repeated passages. By passage 5, the cell numbers had expanded by approximately 1000-fold in the cells of each MPC unit composition (0–10%). Under the osteogenic condition, the cells selected by the MPC polymer coated-plates and cultured in the conventional PS plate ones for a single time (passage 2) more highly expressed the COL1A1 mRNA in the 2–5% MPC than in the 0%, but those by the 1 or 10% MPC polymer-coated plates did not show any significant increase in the COL1A1 expression. The promotion effects of the COL1A1 expression in 2% MPC unit composition continued even at passage 5, although the cells at passage 2 were more sensitive for the osteogenic differentiation than those at passage 5. ALP also peaks at 2-5% MPC unit composition for both passages, although no statistical difference of the ALP expression was detected in passage 2 [Fig. 4(a)]. The ALP enzyme activity was also significantly higher in 5% MPC unit composition than others at passage 2 [Fig. 4(b)].

The expression of the chondrocyte markers in the MPC polymer-selected cells under the chondrogenic conditions was also enhanced in the 2–5% MPC unit composition, as observed during osteogenesis. Responding to the chondrogenic induction, the cells began to express COL2A1, COL10A1, and Sox 9, and especially cells selected by the 2% MPC unit composition showed a prominent expression of all chondrocyte markers not only at passage 2, but even at passage 5 (Fig. 5).

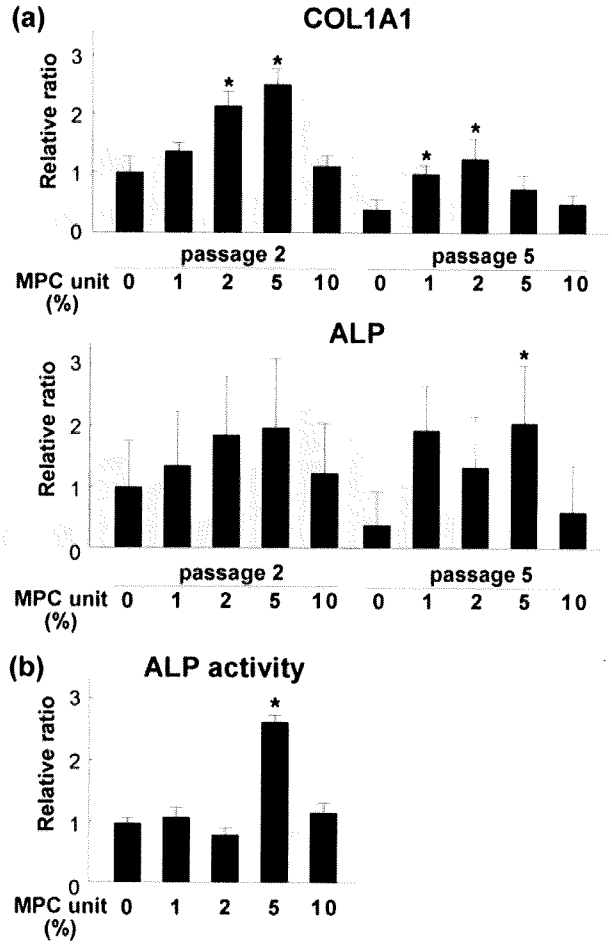

Figure 4. (a) Gene expression of COL1A1 and ALP in the osteogenic induction. Significant expression of COL1A1 gene was found in human MSCs selected by the MPC polymer-coated plates (2–5% unit composition) at passage 2, while the high expression level in the 5% MPC unit composition continued by passage 5. Also, in the ALP expression, the promotion effect was observed in 2–5% MPC unit composition, especially at passage 5. All values are presented as mean plus standard deviation of five samples per group. Statistics were assessed using Dunnett's test (*$p < 0.01$ vs. 0% MPC unit composition). (b) The enzyme activity for ALP in the osteogenic induction. The ALP enzyme activity was also significantly higher in 5% MPC unit composition than others in the rat MSCs at passage 2. All values are presented as mean plus standard deviation of three measurements per group. Statistics were assessed using Dunnett's test (*$p < 0.01$ vs. 0% MPC unit composition).

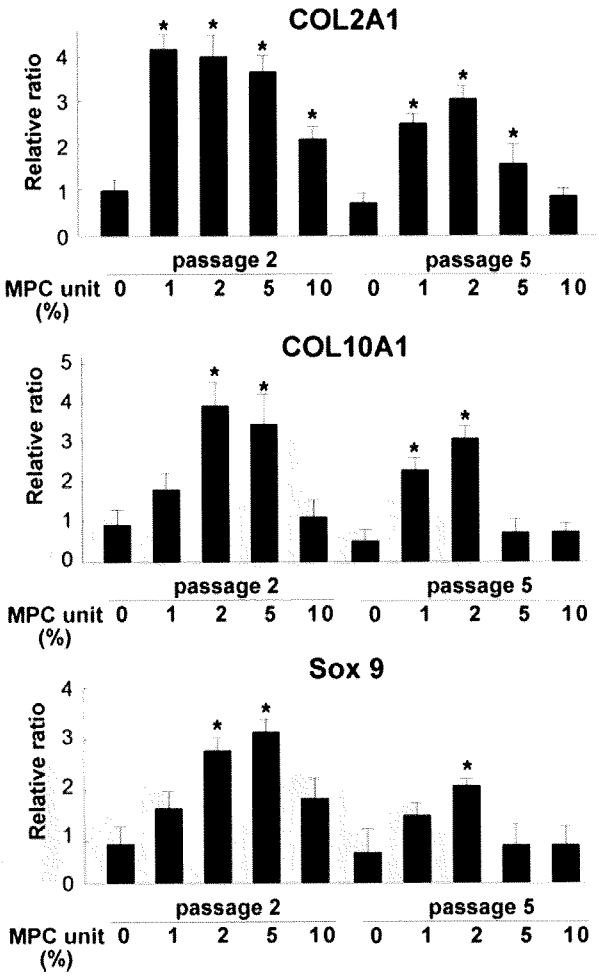

Figure 5. Gene expression of COL2A, COL10A1, and Sox9 during the chondrogenic induction. The expressions of COL2A1, COL10A1, and Sox9 genes peaked at 2–5% MPC unit composition not only at passage 2 but also at passage 5. All values are presented as mean plus standard deviation of five samples per group. Statistics were assessed using Dunnett's test (*$p < 0.01$ vs. 0% MPC unit composition).

DISCUSSION

The adhesion capacity seems to have some association with the cellular activities and functions. Specific adhesion to the laminin and type IV collagen coated on the surface of the culture dishes could select the myogenic cells of the embryonic mouse thigh from fibroblastic cells. Over a brief time period (10–20 min), myoblasts from the embryonic mouse thigh muscle had adhered faster to the laminin than did the fibroblasts from the same tissue, while the latter adhered faster to the fibronectin than the former.[19] Laminin-1 also enriched the osteoblast progenitor cells from rat calvarial cells when they were seeded on the culture wells coated with it. The laminin-1 inhibited cell attachment of the rat calvarial cells, but could select the highly osteogenic lineage according to the difference in the cell adhesiveness to that of the molecule.[20] Thus, through the selection of the cell adhesion to some molecules, a specific cell subpopulation that possesses a high differentiation potency would be concentrated from heterogeneity of the cell sources.

MSC expresses many adhesion-related molecules, like the integrin subunits α4, 5, 6, 8, 9, v/β1, 3, 5, ICAM-1, ALCAM, VCAM-1, SCF, fibronection, E-cadherin, and hyaluronan receptor[21–23] and can be bound to various ligands including laminin and E-cadherin to play biological roles through the cell-to-cell or cell-to-matrix contacts. As examples of the cell-to-cell contact with MSCs *in vivo*, homing functions for the hematopoietic cells of MSCs should be discussed. Through the cell-to-cell contacts with hematopoietic stem cells mediated by VCAM-1, fibronectin, SCF, E-cadherin, or ICAM-1, MSCs secrete extracellular matrix proteins, produce secreted/membrane-bound cytokines and regulate hematopoiesis.[22] MSCs are also recruited and adhered to the damaged tissues in order to participate in tissue repair. These cells can provide cell sources for tissue repair in bone, cartilage, and even skeletal muscle or myocardium that do not directly make contact with bone marrow. Once muscles are injured, the MSCs are delivered to the degenerative muscles from the circulation, are adhered to the lesion, take part in the regenerative process, and provide fully differentiated muscle fibers.[24] In the murine model of cardiac repair following ischemic injury, MSCs were mobilized from bone marrow, homed and generated cardiac myocytes. Among the adhesion molecules of the MSC such as integrin α4, 6, 8, 9, and β1, blockade of the integrin β1 by the neutralizing antibody reduced the total number of MSCs in the infracted myocardium, suggesting that MSCs utilized integrin β1 for cell adhesion to the myocardium and its regeneration.[23]

Thus, MSCs can be bound to various partners via many kinds of adhesion molecules to exert physiological and pathological functions. Although the adhesiveness to some ligands likely selects a cell subpopulation with a high differentiation potency of a certain lineage,[19,20] such a specific selection may have the risk to reduce the multipotency in MSCs. Therefore, we applied the selection system based not on the adhesiveness to specific molecules, but on the general adhesion ability to the MPC polymer-coated plates. As a result, we could enrich the cells to have a high potency of both osteogenesis and chondrogenesis from the crude MSCs.

It has yet remained unknown why the strength of the adhesion ability in MSCs could enhance not the proliferation rate of the cells, but the differential

potential for both osteogenesis and chondrogenesis. Speculating that such multipotent cells may show a stronger adhesion than fibroblastic cells in bone marrow, the MPC polymer-selection due to cell attachment could exclude the fibroblastic ones that possess a lower differentiation potential. This selection probably enriched the cells with high differentiation potential. It implied not that the MPC polymer-coated plates did not induce the phenotype changes in each cell, but that they purified the cell populations by the elimination of fibroblastic cells from the total populations of bone marrow adhesive cells. Therefore, the difference in osteogenic and chondrogenic ability was maintained during the repeated passaging, and the MPC polymer selection could improve cellular potential even after recultivation on PS plates. However, as we do not currently possess the methods to exactly distinguish MSCs from fibroblastic cells using cell surface epitopes, it may be hard to prove that the MPC selection could concentrate the multipotent MSCs from a mixture of the MSCs with fibroblast, by flow cytometry that can exactly exclude the hematopoietic lineage from the MSCs.

MSC can be differentiated into a variety of tissues including bone, cartilage, tendon, fat, heart, muscle or brain, *in vitro* and *in vivo*.[1,8] Autologous MSCs have advantages over embryonic stem cells, regarding the teratocarcinoma formation, immune rejection, or ethical problems. The cell sources have already been used for the treatment of osteogenesis imperfecta, bone/cartilage defects, myocardiac infarction, or skin ulcer.[25–28] Conversely, the MPC polymers have also been already applied in the clinical field for the surfaces of intravascular stents, intravascular guide wires, soft contact lenses, and the artificial lung, all of which were authorized by the United States Food and Drug Administration.[13,14] Thus, the biocompatible polymer is regarded to be approved for safe clinical use.

The MPC selection is as simple as to culture MSCs with MPC polymer-coated plates in the first passage, which would reduce the risks of contamination or mismanagement during the culture procedure. The improvement of the MSCs in purity and multipotency by the MPC polymer selection would provide promising technologies for the next generation-cell therapy that can be applied for more severe and other various diseases. The clinical application of the MPC polymer-selected MSCs is now underway.

References

1. Pittenger MF, Mackay AM, Beck SC, Jaiswal RK, Douglas R, Mosca JD, Moorman MA, Simonetti DW, Craig S, Marshak DR. Multilineage potential of adult human mesenchymal stem cells. Science 1999;284:143–147.
2. Makino S, Fukuda K, Miyoshi S, Konishi F, Kodama H, Pan J, Sano M, Takahashi T, Hori S, Abe H, Hata J, Umezawa A, Ogawa S. Cardiomyocytes can be generated from marrow stromal cells in vitro. J Clin Invest 1999;103:697–705.
3. Kopen GC, Prockop DJ, Phinney DG. Marrow stromal cells migrate throughout forebrain and cerebellum, and they differentiate into astrocytes after injection into neonatal mouse brains. Proc Natl Acad Sci USA 1999;96:10711–10716.
4. Friedenstein AJ, Deriglasova UF, Kulagina NN, Panasuk AF, Rudakowa SF, Luria EA, Ruadkow IA. Precursors for fibroblasts in different populations of hematopoietic cells as detected by the in vitro colony assay method. Exp Hematol 1974;2:83–92.
5. Sekiya I, Larson BL, Vuoristo JT, Cui JG, Prockop DJ. Adipogenic differentiation of human adult stem cells from bone marrow stroma (MSCs). J Bone Miner Res 2004;19:256–264.
6. Colter DC, Sekiya I, Prockop DJ. Identification of a subpopulation of rapidly self-renewing and multipotential adult stem cells in colonies of human marrow stromal cells. Proc Natl Acad Sci USA 2001;98:7841–7845.
7. Smith JR, Pochampally R, Perry A, Hsu SC, Prockop DJ. Isolation of a highly clonogenic and multipotential subfraction of adult stem cells from bone marrow stroma. Stem Cells 2004;22:823–831.
8. Ishii M, Koike C, Igarashi A, Yamanaka K, Pan H, Higashi Y, Kawaguchi H, Sugiyama M, Kamata N, Iwata T, Matsubara T, Nakamura K, Kurihara H, Tsuji K, Kato Y. Molecular markers distinguish bone marrow mesenchymal stem cells from fibroblasts. Biochem Biophys Res Commun 2005;332: 297–303.
9. Pochampally RR, Smith JR, Ylostalo J, Prockop DJ. Serum deprivation of human marrow stromal cells (hMSCs) selects for a subpopulation of early progenitor cells with enhanced expression of OCT-4 and other embryonic genes. Blood 2004; 103:1647–1652.
10. Ueda H, Watanabe J, Konno T, Takai M, Saito A, Ishihara K. Asymmetrically functional surface properties on biocompatible phospholipid polymer membrane for bioartificial kidney. J Biomed Mater Res A 2006;77:19–27.
11. Sawada S, Iwasaki Y, Nakabayashi N, Ishihara K. Stress response of adherent cells on a polymer blend surface composed of a segmented polyurethane and MPC copolymers. J Biomed Mater Res A 2006;79:476–484.
12. Sibarani J, Takai M, Ishihara K. Surface modification on microfluidic devices with 2-methacryloyloxyethyl phosphorylcholine polymers for reducing unfavorable protein adsorption. Colloids Surf B Biointerfaces 2007;54:88–93.
13. Lewis AL, Tolhurst LA, Stratford PW. Analysis of a phosphorylcholine-based polymer coating on a coronary stent pre- and post-implantation. Biomaterials 2002;23:1697–1706.
14. Kihara S, Yamazaki K, Litwak KN, Litwak P, Kameneva MV, Ushiyama H, Tokuno T, Borzelleca DC, Umezu M, Tomioka J, Tagusari O, Akimoto T, Koyanagi H, Kurosawa H, Kormos RL, Griffith BP. In vivo evaluation of a MPC polymer coated continuous flow left ventricular assist system. Artif Organs 2003;27:188–192.
15. Moro T, Takatori Y, Ishihara K, Konno T, Takigawa Y, Matsushita T, Chung UI, Nakamura K, Kawaguchi H. Surface grafting of artificial joints with a biocompatible polymer for preventing periprosthetic osteolysis. Nat Mater 2004;3:829–836.
16. Goda T, Ishihara K. Soft contact lens biomaterials from bioinspired phospholipid polymers. Expert Rev Med Devices 2006;3:167–174.
17. Kato Y, Iwamoto M, Koike T, Suzuki F, Takano Y. Terminal differentiation and calcification in rabbit chondrocyte cultures grown in centrifuge tubes: Regulation by transforming growth factor beta and serum factors. Proc Natl Acad Sci USA 1988;85:9552–9556.

18. Ebisawa K, Hata K, Okada K, Kimata K, Ueda M, Torii S, Watanabe H. Ultrasound enhances transforming growth factor β-mediated chondrocyte differentiation of human mesenchymal stem cells. Tissue Eng 2004;10:921–929.
19. Kuhl U, Ocalan M, Timpl R, von der Mark K. Role of laminin and fibronectin in selecting myogenic versus fibrogenic cells from skeletal muscle cells in vitro. Dev Biol 1986;117:628–635.
20. Roche P, Rousselle P, Lissitzky JC, Delmas PD, Malaval L. Isoform-specific attachment of osteoprogenitors to laminins: Mapping to the short arms of laminin-1. Exp Cell Res 1999;250:465–474.
21. Conget PA, Minguell JJ. Phenotypical and functional properties of human bone marrow mesenchymal progenitor cells. J Cell Physiol 1999;181:67–73.
22. Hall BM, Gibson LF. Regulation of lymphoid and myeloid leukemic cell survival: Role of stromal cell adhesion molecules. Leuk Lymphoma 2004;45:35–48.
23. Ip JE, Wu Y, Huang J, Zhang L, Pratt RE, Dzau VJ. Mesenchymal stem cells utilize integrin beta 1 not CXC chemokine receptor 4 for myocardial migration and engraftment. Mol Biol Cell 2007;18:2873–2882.
24. Ferrari G, Cusella-De Angelis G, Coletta M, Paolucci E, Stornaiuolo A, Cossu G, Mavilio F. Muscle regeneration by bone marrow-derived myogenic progenitors. Science 1998;279:1528–1530.
25. Horwitz EM, Prockop DJ, Fitzpatrick LA, Koo WW, Gordon PL, Neel M, Sussman M, Orchard P, Marx JC, Pyeritz RE, Brenner MK. Transplantability and therapeutic effects of bone marrow-derived mesenchymal cells in children with osteogenesis imperfecta. Nat Med 1999;5:309–313.
26. Quarto R, Mastrogiacomo M, Cancedda R, Kutepov SM, Mukhachev V, Lavroukov A, Kon E, Marcacci M. Repair of large bone defects with the use of autologous bone marrow stromal cells. N Engl J Med 2001;344:385–386.
27. Vojtassak J, Danisovic L, Kubes M, Bakos D, Jarabek L, Ulicna M, Blasko M. Autologous biograft and mesenchymal stem cells in treatment of the diabetic foot. Neuro Endocrinol Lett 2006;27(Suppl 2):134–1371.
28. Fox JM, Chamberlain G, Ashton BA, Middleton J. Recent advances into the understanding of mesenchymal stem cell trafficking. Br J Haematol 2007;137:491–502.

Cartilage-mimicking, high-density brush-like structure confers high durability to cross-linked polyethylene

Running title: High-density brush surface on CLPE

Masayuki Kyomoto, PhD[1,2,4,*], Toru Moro, MD[2,3], Yoshio Takatori, MD[2,3], Hiroshi Kawaguchi, MD[3], Kozo Nakamura, MD[3], Kazuhiko Ishihara, PhD[1]

[1]*Department of Materials Engineering,* [2]*Division of Science for Joint Reconstruction, Graduate School of Medicine, and* [3]*Sensory & Motor System Medicine, Faculty of Medicine, The University of Tokyo, 7-3-1, Hongo, Bunkyo-ku, Tokyo 113-8654, Japan*

[4]*Research Department, Japan Medical Materials Corporation, 3-3-31, Miyahara, Yodogawa-ku, Osaka 532-0003, Japan*

This work was supported by a Health and Welfare Research Grant for Translational Research (H17-005), Research on Medical Devices for Improving Impaired QOL (H20-004) from the Japanese Ministry of Health, Labour and Welfare.

*All correspondence should be addressed to: Masayuki Kyomoto

Research Department, Japan Medical Materials Corporation, 3-3-31, Miyahara, Yodogawa-ku, Osaka 532-0003, Japan

Phone: +81-6-6350-1014, Fax: +81-6-6350-5752

E-mail: kyomotom@jmmc.jp